Master of Science Thesis in Electrical Engineering
Department of Electrical Engineering, Linköping University, 2023

# Model Predictive Control for Ground Source Heat Pumps

## Reducing cost while maintaining comfort

**Charlie Elf and Isak Bokne**

LINKÖPING UNIVERSITY

Master of Science Thesis in Electrical Engineering

**Model Predictive Control for Ground Source Heat Pumps: Reducing cost while maintaining comfort**

Charlie Elf and Isak Bokne

LiTH-ISY-EX--23/5585--SE

Supervisor: **Shamisa Shoja**
ISY, Linköpings universitet
**David Salomonsson**
ALTEN
**Pontus Höjer**
ALTEN

Examiner: **Johan Löfberg**
ISY, Linköpings universitet

*Division of Automatic Control*
*Department of Electrical Engineering*
*Linköping University*
*SE-581 83 Linköping, Sweden*

# Abstract

Today, the control of heat pumps aims to first and foremost maintain a comfortable indoor temperature. This is primarily done by deciding input power based on outside temperature. The cost of electricity, which can be rather volatile, is not taken into account. Electricity price can be provided on an hourly rate, and since a house can store thermal energy for a duration of time, it is possible to move electricity consumption to hours when electricity is cheap.

In this thesis, the strategy used in the developed controller is Model Predictive Control (MPC). It is a suitable strategy because of the ability to incorporate an objective function that can be designed to take the trade-off between indoor temperature and electricity cost into account. The MPC prediction horizon is dynamic as the horizon of known electricity spot prices varies between 12 and 36 hours throughout the day. We model a residential house heated with a ground source heat pump for use in a case analysis. Sampled weather and spot price data for three different weeks are used in computer simulations. The developed MPC controller is compared with a classic *heat curve* controller, as well as with variations of the MPC controller to estimate the effects of prediction and model errors.

The MPC controller is found to be able to reduce the electricity cost and/or provide better comfort and the prioritization of these factors can be changed depending on user preferences. When shifting energy consumption in time it is necessary to store thermal energy somewhere. If the house itself is used for this purpose, variations in indoor temperature must be accepted. Further, accurate modeling of the Coefficient of Performance (COP) is essential for ground source heat pumps. The COP varies significantly depending on operating conditions and the MPC controller must therefore have a correct perception of the COP. Publicly available weather forecasts are of sufficient quality to be usable for future prediction of outside temperature. For future studies, it would be advantageous if better models can be developed for prediction of global radiation. Including radiation in the MPC controller model would enable better comfort with very similar operating costs compared to when the MPC controller does not take radiation into account.

# Acknowledgments

We would like to extend our thanks to our supervisors at ALTEN, Pontus Höjer and David Salomonsson (as well as to the rest of the team). It has been very pleasant working with you this spring and you have always been very supportive and generous with your time and professional knowledge.

*Linköping, June 2023*
*Charlie Elf and Isak Bokne*

# Contents

**Notation** **ix**

**1 Introduction** **1**
1.1 Motivation . . . 1
1.2 Purpose . . . 2
1.3 Problem Formulation . . . 2
1.4 Delimitations . . . 2

**2 Theory** **5**
2.1 Related Work . . . 5
2.1.1 Current Standard Practice . . . 5
2.1.2 Heat Pump Control Strategy Research . . . 6
2.1.3 Building Modeling . . . 7
2.2 Heat Pump . . . 7
2.2.1 Heat Pump Types . . . 8
2.2.2 Coefficient of Performance . . . 8
2.3 Heat Flow . . . 9
2.3.1 Conduction . . . 9
2.3.2 Convection . . . 10
2.3.3 Radiation . . . 10
2.3.4 Heat Conservation for the Steady Flow of a Fluid in a Tube 10
2.4 Electricity Market . . . 10
2.5 Optimal Control . . . 13
2.5.1 Model Predictive Control . . . 13
2.5.2 MPC Problem Formulation . . . 14
2.5.3 MPC Algorithm . . . 15

**3 Modeling and Control** **17**
3.1 Data Acquisition . . . 17
3.2 Overall System Description . . . 17
3.3 House Model . . . 18
3.4 Heat Pump Model . . . 20
3.4.1 Identification of the COP Model . . . 20

3.5 Controller . . . . . 23
3.5.1 Heat Curve Controller . . . . . 23
3.5.2 MPC Controller . . . . . 27
3.6 Weather Prediction . . . . . 32
3.6.1 Temperature Forecast Quality . . . . . 32

**4 Benchmarking and Results** **35**
4.1 Analysed Cases . . . . . 35
4.1.1 Period 1: 7 Days with Highly Varying Spot Prices . . . . . 36
4.1.2 Period 2: 7 Days with High Spot Prices and Cold Weather . 36
4.1.3 Period 3: 7 Days with Low Spot Prices, Warm Weather and High Prediction Errors . . . . . 36
4.2 Benchmarking . . . . . 38
4.3 Performance . . . . . 39
4.3.1 Period 1 . . . . . 39
4.3.2 Period 2 . . . . . 40
4.3.3 Period 3 . . . . . 42
4.4 Control Signal Characteristics . . . . . 43

**5 Discussion and Conclusion** **47**
5.1 Constant vs. Varying COP . . . . . 47
5.2 Sensitivity to Forecast Errors . . . . . 48
5.3 Model Complexity . . . . . 48
5.4 Forecasting Radiation . . . . . 50
5.5 Overdimensioned Heating System . . . . . 50
5.6 Comfort vs. Cost . . . . . 50
5.6.1 Weight . . . . . 50
5.6.2 Soft Constraint . . . . . 51
5.7 Control Signal Characteristics . . . . . 51
5.8 Implementation Feasibility . . . . . 52
5.8.1 Heating System Model . . . . . 52
5.8.2 House Model . . . . . 52
5.8.3 Computing Power . . . . . 53
5.8.4 Spot Price Data . . . . . 53
5.9 Conclusion . . . . . 53
5.10 Future Work . . . . . 54

**A Controller Performance Plots** **57**

**B Radiation Model** **71**
B.1 Radiation as a Function of Sunshine . . . . . 71
B.2 Radiation as a Function of Cloudiness . . . . . 72

**Bibliography** **77**

# Notation

### Abbreviations

| Abbreviation | Description |
|---|---|
| COP | Coefficient of Performance |
| LTI | Linear Time Invariant |
| MILP | Mixed Integer Linear Programming |
| MPC | Model Predictive Control |
| RC | Resistance Capacitance |
| SCOP | Seasonal Coefficient of Performance |
| SMHI | Swedish Meteorological and Hydrological Institute |
| ZOH | Zero-Order Hold |

### Notations

| Notation | Description |
|---|---|
| $A$ | Area |
| $c_e$ | Spot price |
| $c_p$ | Specific heat capacity |
| $C$ | Thermal capacitance |
| $G$ | Solar radiation |
| $h$ | Heat transfer coefficient |
| $k$ | Thermal conductivity |
| $L$ | Thickness |
| $P$ | Input power |
| $Q$ | Heat |
| $\dot{Q}$ | Heat flow |
| $R$ | Thermal resistance |
| $R_\epsilon$ | Soft constraint cost coefficient |
| $\rho$ | Density |
| $T$ | Temperature |
| $\dot{V}$ | Volumetric flow rate |
| $W$ | Work |

# 1 Introduction

Currently, the most common method for indoor climate control in buildings with water bound radiator systems is the utilization of a *heat curve*. The aim of this method is to provide a constant indoor climate regardless of outside temperature. It does however not take electricity price or future weather into account. There are however control techniques which could possibly make advantageous use of this information. One of them is Model Predictive Control (MPC). This method uses an objective function which can be designed to take both comfort and electricity cost into account. It also simulates the system during a set horizon for which future electricity price data and weather forecasts can be used.

## 1.1 Motivation

Long term there is a need to lower the greenhouse gas emissions. According to the Paris agreement, EU is committed to lower the emissions of greenhouse gas by 55% until 2030 compared to 1990 [1]. Lowering energy consumption is a way to contribute towards achieving this goal. In Sweden, production of electricity primarily comes from fossil free energy sources (wind, hydro, nuclear) [2]. For comparison, in Germany most of the electricity production comes from wind power and coal-fired power plants. Electricity produced by wind power is generally cheaper than electricity produced by burning coal [3]. Hence, when there is enough wind power production to meet the demand the electricity price tends to go down. It would thus be beneficial both economically and environmentally to make use of low electricity prices.

As 27% of space heating and hot water heating in Sweden in 2021 was powered by electricity (including heat pumps), it is of great interest to study ways to provide efficient control for these applications. In 2019, 60% of one- and two-dwelling buildings in Sweden used heat pumps for heating [4].

## 1.2 Purpose

This thesis aims to propose a solution to reduce the energy cost for spacial heating with ground source heat pumps using modern automatic control methods. Electricity prices are normally supplied per day but as hourly prices are becoming more popular there is potential for customers to make use of it in order to reduce cost. The aim is not to reduce total energy consumption, but rather to control the time and magnitude of energy use in heat pumps for spacial heating to reduce the energy costs. Reducing energy cost would benefit both consumers and society as the consumer saves money and the strain on the electricity grid is reduced when consumption is moved to off-peak hours.

While it is an advantage if cost can reduced, comfort is also important. After all, the main purpose of indoor heating is to make the indoor climate comfortable. The solution must therefore also provide a comfortable indoor climate.

## 1.3 Problem Formulation

Currently, heat pumps for water-bound heating systems determine the temperature of the water going into the system, the *flow line temperature*, as a function of outside temperature. Since they do not take weather forecasts and the cost of electricity into account there is an opportunity to explore if doing so could be beneficial. Modern control strategies enable the usage of such data and thus the following question arises:

> Can electricity cost for a heat pump be reduced, while maintaining comfort, by utilizing optimal control strategies in combination with electricity price data and weather prediction?

## 1.4 Delimitations

#### Only simulations

The experiments are only performed in simulations, no experiments are performed on a real system. This was decided early as a real-world system was deemed to require significant time for the implementation, time which would yield little academic value.

#### Available data

This thesis uses electricity price data supplied by Nord Pool and weather data from the Swedish Meteorological and Hydrological Institute (SMHI). Norrköping in Sweden was chosen as the place of study due to good availability of data. Some non-confidential data was supplied by NIBE.

### Simplified house model

House models do not take factors such as furniture, people, opening and closing doors, lights or other electric appliances into account. Moreover, walls and windows will be modeled as flat surfaces assuming steady-state heat flow and isotropic materials to enable the usage of the equations stated in Section 2.3.

### Heat pump type

Only one ground source heat pump is modeled. There are also other types of heat pumps, but those are not examined in this thesis.

### Heat pump models

Real-world heat pumps are complex, hence when modeling the internal system of a heat pump simplifications has been made. For example, valves, sensors, and pumps that are not expected to affect the result significantly may be neglected and the focus was on the energy input and output of the heat pump.

### No hot water production

Heat pumps are usually used to heat warm water, which means that the heat pump may not be available for heating radiators at all times. This is not taken into account in this thesis. Instead, it is assumed that the heat pump is always able to heat the radiators.

# 2

# Theory

In this chapter, current standard practice of heat pump control is examined. This is followed by a presentation of research into alternative methods for heat pump control. Also, research on building modeling is reviewed. Further, theory used in this thesis, such as heat pump Coefficient of Performance (COP), heat flow, the electricity market, and optimal control is presented.

## 2.1 Related Work

Climate control in buildings has for a long time been a subject with relatively little innovation. Control practices has remained constant as current techniques can provide a comfortable indoor climate. Focus has been on improving energy consumption by improving building practices, such as better insulation and reuse of thermal energy in outgoing ventilation air.

Recently however, there has been an increasing amount of research into building climate control. This includes research on how control-oriented models of buildings can be constructed, as well as how predictions of future weather and energy price can be used for increased comfort and/or reduced energy cost.

### 2.1.1 Current Standard Practice

The power output from a heat pump can be varied by changing the temperature or the mass flow rate of the water going out from the heat pump and into the radiator system. The temperature of the water at this point is known as the *flow line temperature*. In general, the flow line temperature is determined as a function of outside temperature, known as the *heat curve*. The heat curve aims to yield a constant indoor temperature independent of the outside temperature. The heat curve can be shifted to adjust the indoor temperature. This can be done

either manually or by utilizing an indoor temperature sensor and letting a control system set the heat curve. If done manually, the heat curve is set for the highest desired temperature in the house, where the radiators are also generally overdimensioned. The temperature can then be adjusted at the thermostats on the radiators [5].

### 2.1.2 Heat Pump Control Strategy Research

Research is being performed to evaluate how heat pump control can be developed. In general, there is a shift from just controlling the reference indoor temperature, to weighing in more factors such as electricity cost.

Studies regarding the use of machine learning and AI for heat pump control have been done. S. Noye et al. [6] concludes that it would be possible and beneficial to use AI in an on-line application because of the complexity and difference between real-world situations. This is however a field that needs further studies.

Using MPC for the purpose of minimizing electricity cost for heat pumps has been studied previously. Kajgaard et al. [7] found that it was possible to reduce the electricity cost for a typical danish house by 7% in a given month (price and weather data from February 2012). The study found that the potential savings are inversely correlated with required comfort. A higher acceptance for temperature variation makes larger savings possible.

Heat pumps in conjunction with other components such as thermal storage tanks and solar cells was studied by R. Yumrutaş and M. Ünsal [8]. Solar energy was used for heating water in a storage tank buried below the ground. A heat pump was then used to supply sufficient water temperature for spatial heating with radiators. P. Wu et al. [9] performed a case study using a water tank as thermal storage together with a heat pump. The heat pump operated only during times of relatively high ambient temperature to heat the building and charge the storage tank. During times of low ambient temperature the heat pump was switched off and the thermal storage tank discharged to maintain indoor temperature. The study showed that the method could maintain the indoor temperature within the range 21°C - 23°C while the average ambient temperature was between −9.3°C and 11.3°C. They recorded an increase of seasonal Coefficient of Performance (SCOP) of 26.1% and 14.0% daily average COP. Huchtemann [5] found that having a thermal storage in the form of a water tank had a much higher influence on the heating system inertia than the materials used in building walls.

Heat pump manufacturers have implemented other means of reducing energy cost. These may have limited foundation in theory, but can still provide significant savings. For example, NIBE has a function called *Smart Price Adaption* which offsets energy usage to hours when the electricity price is lower [10]. These algorithms are however generally confidential and therefore hard to study academically.

### 2.1.3 Building Modeling

While MPC has shown to be effective for climate control of a building, it has not been widely used. Oldewurtel et al. [11] argues that this is due to the difficulties/costs associated with obtaining a model of an individual building, and the fact that energy has been cheap, thus not making the investment pay off. Using MPC also introduces requirements on the type of model that is used. Computer aided modeling tools such as TRNSYS, EnergyPlus, and ESP-r, which are often used for modeling buildings, create models which are very complicated and thus not easily usable for control purposes [12].

If there is ample measurement data available for the building, it is preferred to use a purely statistical model [12]. Some statistical methods are presented in [13], including *sub-space methods*, *prediction error methods*, and *MPC relevant identification*. These will not be considered in this thesis due to the lack of measurement data.

One technique which is useful for modeling buildings for control purposes is Resistance-Capacitance (RC) modeling. Similar to an electrical circuit, the thermal resistance can be modeled as a resistor and the thermal capacity as a capacitor [12]. These models can easily be made more or less complex depending on requirements. They are also very easy to describe analytically and are therefore easy to use for MPC. This technique has been used by several projects for using MPC for heating control, at among others UC Berkley, ETH Zürich, and KU Leuven [13].

## 2.2 Heat Pump

The objective of a heat pump is to move thermal energy from one place to another, which is realized in a compressor cycle. The benefit compared with other types of heat generation is that much of the desired thermal output does not have to be converted from another form of energy. Instead, thermal energy can be moved from a place where there is an abundance of thermal energy to the place where it is desired.

Figure 2.1 illustrates the working principle of the compressor cycle. The system contains a fluid which carries thermal energy. The compressor raises the pressure of the fluid under constant entropy. The fluid then passes through the condenser which emits heat to its surrounding environment, for example by passing a heat exchanger and transferring heat to water which heats radiators in a building. After this, the fluid passes through the expansion valve causing the pressure and temperature to drop. At last, thermal energy is transferred from the source to the fluid as it passes the evaporator [14]. Thermal energy can be transferred to the evaporator with a radiator in the case of an air source heat pump or with a heat exchanger in the case of a ground source heat pump.

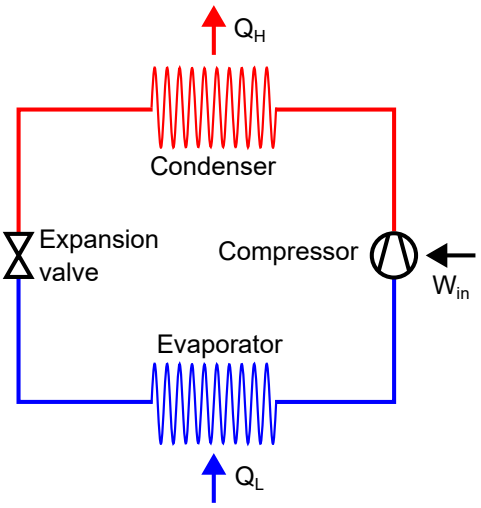


***Figure 2.1:*** *Schematics of a compressor cycle.*

### 2.2.1 Heat Pump Types

Different means can be used to move thermal energy to the evaporator and to extract thermal energy from the condenser. In a ground source heat pump, a fluid which circulates in pipes in the ground outside the building transfers thermal energy to the evaporator through a heat exchanger. Energy can also be transferred to the evaporator by forced convection, where the evaporator is a radiator over which a fan blows air. In this case, the evaporator can be located either outside the building, or inside the building if it is an exhaust air heat pump.

### 2.2.2 Coefficient of Performance

The performance of a heat pump is evaluated by the Coefficient of Performance (COP). The COP is the factor between heat output $Q_H$ and work input $W_{in}$ [14] and is

$$COP = \frac{Q_H}{W_{in}} \tag{2.1}$$

The COP is not constant for a heat pump but changes depending on operating conditions. Current state of the art residential ground source heat pumps can have COP-values around 4 to 5 [15]. In specification sheets for heat pumps, COP is defined for specific operating conditions. These operating conditions do however not represent the usual operating conditions. To enable better comparison between heat pumps, seasonal COP (SCOP) has been defined in standard EN 14825:2022 [16] as

$$SCOP = \frac{Q_H}{Q_{HE}} \tag{2.2}$$

where $Q_H$ is the reference annual heating demand and $Q_{HE}$ is the annual energy consumption for heating. SCOP is thus the average COP for the whole year.

## 2.3 Heat Flow

There are three basic types of heat flow: conduction, convection, and radiation. Conduction takes place within substances as more energetic particles transfer heat to less energetic adjacent ones. Convection is the heat flow within a fluid in motion. Radiation is energy which is emitted from objects in the form of electromagnetic waves [14].

The models for heat flow presented in this section are valid for steady state. The system in this thesis will not be in steady state, but is expected to be so slow that these models represent reality good enough.

### 2.3.1 Conduction

In the context of this thesis, conduction takes place within the walls, roof, and in the ground surrounding a house. The heat flow through a homogeneous wall is [14]

$$\dot{Q}_{cond,wall} = kA\frac{T_1 - T_2}{L} \tag{2.3}$$

where $k$ is the thermal conductivity, $A$ is the wall area, $L$ is the thickness of the wall, $T_1$ is the temperature on the high temperature side and $T_2$ is the temperature on the low temperature side.

Thermal resistance can be defined

$$R_{wall} = \frac{L}{kA} \tag{2.4}$$

such that

$$\dot{Q}_{cond,wall} = \frac{T_1 - T_2}{R_{wall}} \tag{2.5}$$

The heat flow in a wall consisting of several layers with different thermal conductivity and thickness can be calculated similarly to how current is calculated in an electrical circuit with resistors connected in series. The heat flow for a wall with N layers is then

$$\dot{Q}_{cond,wall} = \frac{T_1 - T_2}{R_{wall,1} + R_{wall,2} + ... + R_{wall,N}} \tag{2.6}$$

where $T_1$ and $T_2$ is the temperatures on the surface of the high temperature side and the low temperature side of the whole wall, respectively. Thermal resistance is evaluated for each layer of the wall.

### 2.3.2 Convection

Convection is the heat flow which takes place in a fluid in bulk motion [14]. Convection is referred to as *natural* if the motion is caused by temperature differences within the fluid and as *forced* if the motion is caused by external factors such as a fan.

For the convective heat flow between a surface such as a wall and a fluid, Newton's law of cooling states that [14]

$$\dot{Q}_{conv} = hA(T_w - T_\infty) \tag{2.7}$$

where $h$ is the heat transfer coefficient of the fluid, $A$ is the area of the wall, $T_w$ is the temperature on the surface of the wall, and $T_\infty$ is the temperature in the surrounding fluid. The thermal resistance for convection can be written

$$R_{conv} = \frac{1}{hA} \tag{2.8}$$

### 2.3.3 Radiation

The heat flow to a surface by global radiation is

$$\dot{Q}_{rad} = AG \tag{2.9}$$

where $A$ is the area of the surface and $G$ is the global radiation, i.e., radiation from the sun hitting a surface on earth, measured in $W/m^2$.

### 2.3.4 Heat Conservation for the Steady Flow of a Fluid in a Tube

If a fluid is in steady flow in a tube, the heat flow to or from the fluid is [14]

$$\dot{Q} = \rho c_p \dot{V}(T_2 - T_1) \tag{2.10}$$

where $\rho$ is the density of the fluid, $c_p$ is the specific heat capacity of the fluid, $\dot{V}$ is the volumetric flow rate, $T_1$ is the temperature of the water at the inlet of the tube, and $T_2$ is the temperature of the water at the outlet of the tube.

## 2.4 Electricity Market

The price which Swedish consumers pay for electricity is made up of several different fees and taxes. The consumer price consists of spot price, emission allowances, and energy tax. The proportions between these can vary depending on the spot price, however, in January 2023 each of those constituted about one third of the consumer price. The consumer price also includes an electricity certificate which constitutes about 1% of the consumer price. On top of the consumer price, the grid owner charges a fee for using the grid [17]. These fees are regulated by the Swedish Energy Markets Inspectorate (Ei). On July 1 2022, Ei imposed new grid tariffs which should be implemented before January 1 2027. These tariffs

will be higher for higher power consumption, aiming to promote the consumer to use electric power more evenly throughout the day and thus reducing their peak power consumption [18]. Finally, all of these fees are subject to 25% VAT, known as moms in Sweden.

Historic and future spot price data is available at Nord Pool [19]. Bidding on the day-ahead trading market Elspot is done until 12:00 CET each day. The spot prices of each bidding area for every hour the following day is then announced at 12:45 CET or later at Nord Pool.

Norrköping, which is the geographical location for the case study in this thesis, is located in price zone SE3. The spot price in this zone has historically been higher during the autumn and winter. Figure 2.2 shows the average price for each week during the period 2011 - 2021.

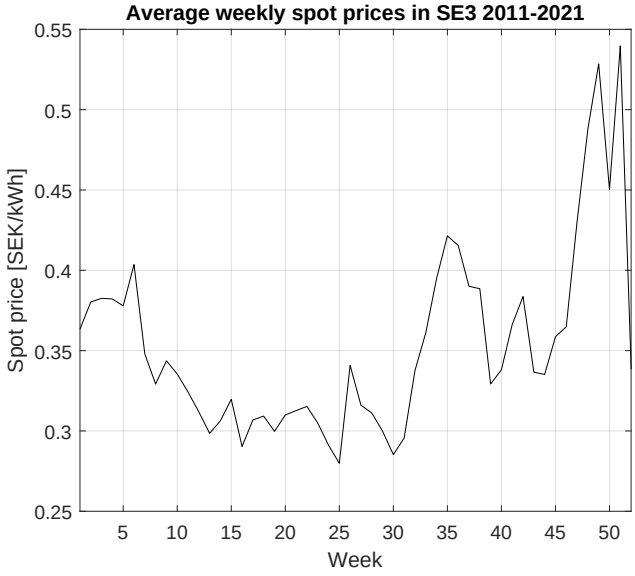


***Figure 2.2:*** *Weekly average spot prices of SE3 for the 11 year period 2011-2021.*

The electricity prices rose during 2021 and 2022. See Figure 2.3.

The spot price is generally higher during the day than during the night. On average it peaks in the morning around 08:00 CET and in the evening around 17:00 - 18:00 CET. See Figure 2.4.

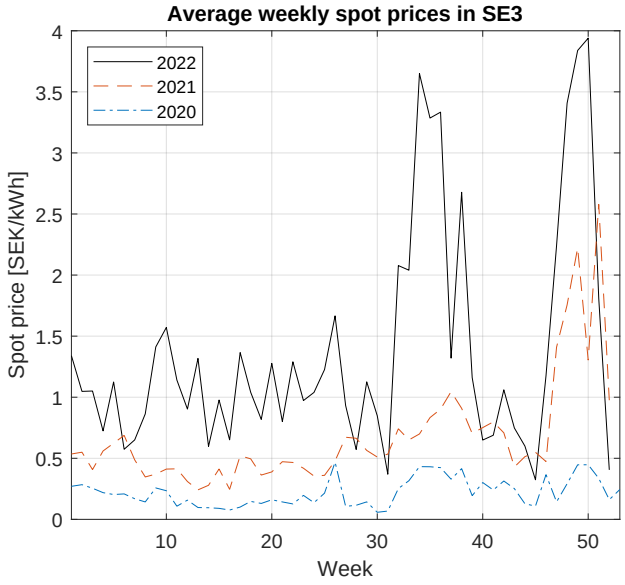


***Figure 2.3:*** *Weekly spot prices of SE3 for the years 2020, 2021, and 2022.*

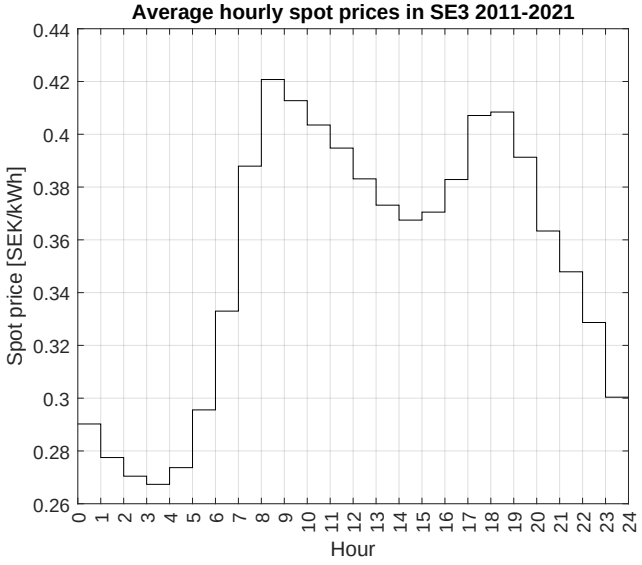


***Figure 2.4:*** *Hourly average spot prices in SE3 for the 11 year period 2011-2021.*

## 2.5 Optimal Control

In optimal control the aim is to control a system such that an objective is optimized. As this thesis aims to find a control strategy for heat pumps such that electricity cost is minimized while comfort is maintained it is fair to say that this is an optimal control problem.

### 2.5.1 Model Predictive Control

Model Predictive Control (MPC) is an optimal feedback control method that utilizes a dynamic model of the system under control to make predictions of how the system will behave over a finite horizon. The predictions are used together with an objective function which is optimized. The objective function is generally chosen to be minimizing some value or maximizing efficiency while being subject to specified constraints. The solution to the optimization is what generates the control signal [20].

When making the predictions of future states, the controller uses a feedback of the current state which is either measured and/or estimated. The predictions over the finite horizon creates a sequence of control signals which will give the final state. The sequence that optimizes the objective function is used and the first control signal is chosen and applied for a specified time period. The process is then repeated [20].

#### Dynamic model

When predicting the future state of the system, the dynamic model is used. It is a mathematical representation of the system under control. In discrete time, with the time step $T_s$, it is often written on state-space form [20]

$$\begin{aligned} x_{k+1} &= Ax_k + Bu_k + Ew_k \\ y_k &= Cx_k + Du_k \\ z_k &= Mx_k \end{aligned} \tag{2.11}$$

where $x_k \in \mathbb{R}^n$, $u_k \in \mathbb{R}^m$, $w_k \in \mathbb{R}^p$, $y_k \in \mathbb{R}^q$, and $z_k \in \mathbb{R}^r$ are the system states, control signal, disturbance, system output signal, and measured signal to control. Predictions are then produced by using the model in Equation (2.11) to simulate time steps forward.

#### Objective function

The objective function is used to specify the performance criterion of the controller. The definition of the objective function decides in what sense the control signal is optimal. The function often includes some state of the system and the control signal in some way. For an MPC controller a prediction horizon ($N$) is included. A general description of an objective function is specified in Equation

(2.12) where $z \in \mathbb{R}^r$ is the measured state(s) and $u \in \mathbb{R}^m$ is the control signal(s) [20].

$$J_N(k) = \sum_{j=0}^{N-1} \ell(z_{k+j|k}, u_{k+j|k}) \tag{2.12}$$

For example, in an application where deviation of $y \in \mathbb{R}$ from a reference $r \in \mathbb{R}$ is to be minimized, and penalties $\gamma \in \mathbb{R}$ and $\delta \in \mathbb{R}$ are applied on the error and input signal, the objective function may be

$$J_N(k) = \sum_{j=0}^{N-1} \gamma |y_{k+j|k} - r_{k+j|k}| + \delta |u_{k+j|k}| \tag{2.13}$$

#### Constraints

An advantage of using MPC is the ability to incorporate system constraints when optimizing [20]. Systems are often limited with regards to the control signal ($u$). For example, a constraint on $u$ can be given as

$$u \in [u_{min}, u_{max}]$$

Constraints can be applied to multiple signals in the control problem. For example, keeping a system state below some value, limiting control signal change rate, and deviation from a reference. They can either be hard or soft meaning that a hard constraint is not allowed to be violated. A soft constraint is a constraint that may add a penalty to the objective function if it is to be violated. It often contains a slack variable which is equal to zero as long as the soft constraint is not violated and thus do not add anything to the objective function.

### 2.5.2 MPC Problem Formulation

With an objective function, constraints, and the dynamic model, a simple illustrative MPC problem can be formulated according to Equation (2.14). $w$ is predicted disturbances made at the time $k$. More constraints may be added to the control problem depending on design criteria.

$$\begin{aligned}
\min_{u} \quad & \sum_{j=0}^{N-1} \gamma |z_{k+j|k} - r_{k+j|k}| + \delta |u_{k+j|k}| \\
\text{s.t.} \quad & u_{k+j|k} \in [u_{min}, u_{max}] \quad \forall j = 0, ..., N-1 \\
& z_{k+j|k} = M x_{k+j|k} \quad \forall j = 0, ..., N-1 \\
& x_{k+j+1|k} = A x_{k+j|k} + B u_{k+j|k} + E w_{k+j|k} \quad \forall j = 0, ..., N-1
\end{aligned} \tag{2.14}$$

### 2.5.3 MPC Algorithm

The MPC is then implemented according to Algorithm 2.1.

**Algorithm 2.1** MPC

1. Measure $x_k$
2. Calculate $u$ by solving the optimization problem (2.14)
3. Apply the first element of $u$ as control signal
4. Update the time $k := k + 1$
5. Go to step 1

# 3

# Modeling and Control

Included in this chapter is a description of the way the house used in the simulations is modeled. The house structure used is described and a state-space representation is produced. The heat pump is modeled using data from a heat pump operating in the real world. There are two controllers developed of which one is a baseline heat curve controller and the other is an MPC controller. Finally the weather forecasts used in the controller is analysed and evaluated.

## 3.1 Data Acquisition

The simulations are not run in real time, but for dates in the past. This means that the simulation time is only limited by computing power, thus enabling simulations to run much faster than real time. For this reason, historic weather data is collected from the SMHI open data source. Two types of weather data are collected; observation data and forecasts. Observation data is easily collected for temperature, wind speed, and solar radiation.

It was not possible to obtain historic weather forecasts from SMHI. For this reason, forecasts were sampled once every hour between 2023-01-24 and 2023-02-15. These dates are therefore the available time window on which simulations can be run.

Historic electricity spot prices are provided from Nord Pool [19], that provides this data for free for academic purposes.

## 3.2 Overall System Description

The system includes a controller, a heat pump, and a house. Because of the way the two different heat pump controllers work, two systems are developed. The

heat curve controller takes the indoor reference temperature ($r$) and outside temperature ($T_{out}$) as inputs and calculates the electrical power ($u$) needed for the heat pump with regards to maintaining the temperature at the chosen reference. The heat pump converts the electrical input power to heat flow ($\dot{Q}_H$) which is transferred to the house model. The house model is a state-space representation derived using RC modeling with the indoor temperature ($T_{in}$) as the measured output. Outside temperature ($T_{out}$) and solar radiation ($G$) are considered disturbances that affect the house through walls and windows. A block diagram of the system using the heat curve controller is shown in Figure 3.1.

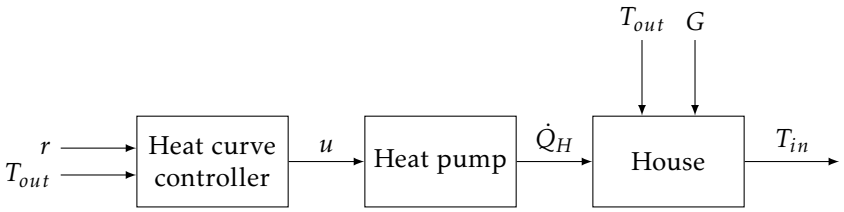


***Figure 3.1:*** *System overview when using the heat curve controller.*

The system design, where MPC instead of the standard heat curve controller is used, takes some additional inputs to the controller. The inputs are indoor reference temperature ($r$), electricity cost ($c_e$), the current indoor temperature ($T_{in}$), and the outside temperature weather forecast ($T_{out,forecast}$). See Figure 3.2. The electricity cost and weather forecasts are vectors of between 12 and 36 elements.

The acquired data is provided to the controller in hourly intervals. The spot price is fixed for every whole hour while the temperature data is interpolated for each time step. This is done to reflect reality, where spot price is fixed for every hour, while the weather is of course changing continuously.

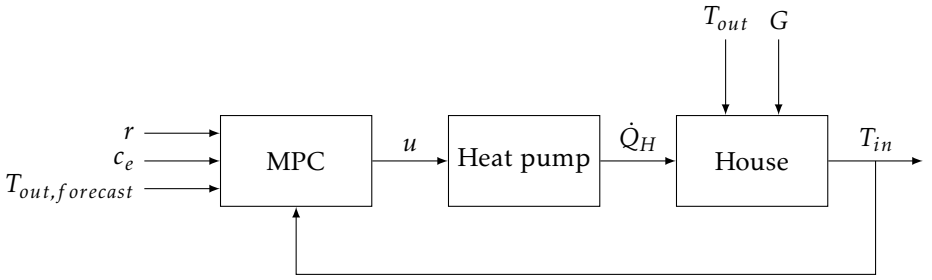


***Figure 3.2:*** *System overview when using the Model Predictive Controller.*

## 3.3 House Model

Modeling of the house is done using RC modeling, depicted in Figure 3.3. Here, $R_e$ represents the thermal resistance between the outside temperature and the

envelope. The envelope is the encapsulation of the house, including the walls and the roof. $R_e$ is including heat flow in the form of convection between outside air, solar radiation on the outside walls, and conduction inside the envelope. $R_i$ is the thermal resistance between the envelope and the indoor temperature including convection between the inside wall and air, solar radiation through the windows, and conduction in the wall. Between the thermal resistances, there is a capacitor, $C_e$ representing the thermal mass of the envelope which also allows for an envelope temperature state, $T_e$. $C_i$ is the interior thermal capacitance. $\dot{Q}_H$ represents the heat flow output from the heat pump into the interior. Choosing to model this as a second order state-space model provides a way to include solar radiation heat flow on both the outside walls ($GA_{wall}$) and through the windows ($GA_{window}$).

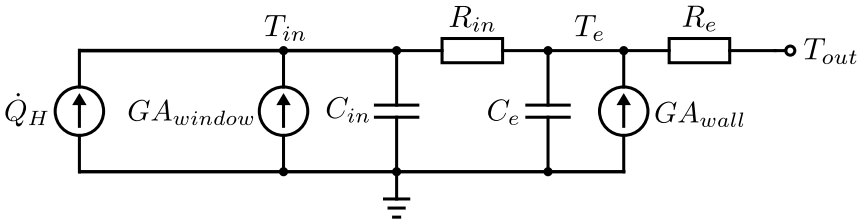


***Figure 3.3:*** *Two state RC-model.*

To use the state-space model in simulation, values for resistances and capacitances have to be included. These are specific for every house and can be found either analytically through very specific knowledge about the house components and material or experimentally using parameter estimation. Doing such experiments requires a house where it is possible to control factors such as heating, and having doors and windows closed. Also, the house should not be inhabited to minimize the risk of errors. This is not within the scope of this thesis and values from a danish study [7] are used. They used parameter estimation to find the resistance and capacitance of a typical danish house with a first order state-space model. The average values from five different experiments were $R = 5.3 \cdot 10^{-3}$ °C/W and $C = 24.5 \cdot 10^6$ J/°C. In our application with a second order system we divide the resistance and capacitance between the inside and envelope with a 1:1 ratio resulting in $R_i = R_e = 2.65 \cdot 10^{-4}$ °C/W, $C_i = C_e = 12.25 \cdot 10^6$ J/°C.

### State-space house model

From the RC-model in Figure 3.3 a state-space model with two states, indoor temperature ($T_{in}$) and envelope temperature ($T_e$) representing the temperature on the surface of the outside wall, is derived. $T_{in}$ is measured while $T_e$ is not. The controlled input signal, heat flow ($\dot{Q}_H$), and two measured disturbances, outside temperature ($T_{out}$) and solar radiation ($G$), affect the house. This gives the differential equations

$$\dot{T}_{in} = \frac{1}{C_{in}R_{in}}(T_e - T_{in}) + \frac{1}{C_{in}}\dot{Q}_H + \frac{A_{window}}{C_{in}}G \tag{3.1}$$

$$\dot{T}_e = \frac{1}{C_e R_{in}}(T_{in} - T_e) + \frac{1}{C_e R_e}(T_{out} - T_e) + \frac{A_{wall}}{C_e} G \tag{3.2}$$

The differential equations can be written on state-space form (in continuous time, unlike in section 2.5.1 where it was written in discrete time.)

$$\dot{x} = Ax + Bu + Ew$$
$$y = Cx + Du$$

where

$$x = \begin{bmatrix} T_{in} \\ T_e \end{bmatrix}, \quad u = \begin{bmatrix} \dot{Q}_H \\ 0 \end{bmatrix}, \quad w = \begin{bmatrix} T_{out} \\ G \end{bmatrix}$$

$$A = \begin{bmatrix} -\frac{1}{C_{in}R_{in}} & \frac{1}{C_{in}R_{in}} \\ \frac{1}{C_e R_{in}} & -\frac{1}{C_e R_{in}} - \frac{1}{C_e R_e} \end{bmatrix}, \quad B = \begin{bmatrix} \frac{1}{C_{in}} \\ 0 \end{bmatrix}, \quad E = \begin{bmatrix} 0 & \frac{A_{window}}{C_{in}} \\ \frac{1}{C_e R_e} & \frac{A_{wall}}{C_e} \end{bmatrix}$$

$$C = \begin{bmatrix} 1 & 0 \end{bmatrix}, \quad D = 0$$

## 3.4 Heat Pump Model

The heat pump is modelled as a function $\dot{Q}_H = f(P_{in})$. The internal dynamics of the heat pump are thereby not taken into account. There are several reasons for this. Primarily, this is done to make the model less complex and piecewise linear. The relationship between electrical input power and heat output power is nonlinear, as COP changes depending on operating conditions.

COP can be modelled as a function of source and flow temperature. The source temperature is the temperature of the thermal fluid from the ground source, while the flow temperature is the temperature of the fluid going into the radiator system, measured directly after the heat pump. Source temperature can be assumed to be constant, but flow temperature is correlated to input power. Introducing flow temperature as a state in the model would in this case mean that the input heating power would be a factor of a state and the input electrical power.

However, as the indoor temperature is maintained around 21°C, the heating power in a specific system will be relatively constant for specific flow temperatures. This means that for each specific system, it is possible to derive a function $\dot{Q}_H = f(P_{in})$. The nonlinearity will then be contained to the input, i.e. $\dot{x} = Ax + Bf(u) + Ew$.

### 3.4.1 Identification of the COP Model

Sensor readings were retrieved from a heat pump which operates in a single family home. The readings were sampled in intervals of 5 minutes between 2022-12-

21 and 2023-03-16. The following signals were sampled: *input power, brine temperature, condenser temperature, return line temperature and volumetric flow*. The input power does not include losses before the inverter which means that some losses will be disregarded. The samples are filtered such that only readings for when the heat pump is in pure heating mode are used (the heat pump can also heat tap water which is not of interest here). Further, only samples with input power above 700 W, brine temperatures between 3 and 7 °C, and with flows over 5 l/min are included. This was done after recommendations from the supervisors at ALTEN, in order to not include unordinary readings which might skew the result. The selected samples have brine temperatures with an average of 4.24 °C and a variance of 0.74 °C. The heating power at each sample can be calculated using Equation (2.10). Properties for water ($\rho_{water}$ and $c_{p,water}$) are used as this is the fluid used in the radiator system. The heating power is the difference between the outgoing heat flow (calculated using the condenser temperature) and the return heat flow, see Equation (3.3).

$$\dot{Q}_H = \rho_{water} c_{p,water} \dot{V} (T_{condenser} - T_{return}) \tag{3.3}$$

Figure 3.4 shows the samples with their respective measured input power $P_{in}$ and calculated heat output $\dot{Q}_H$. In the operating region [700, 3500] W, an affine correlation between $P_{in}$ and $\dot{Q}_H$ can be identified. A model $\dot{Q}_H = kP_{in} + m$ is fitted to the data by using the least squares method. For the case that $P_{in} = 0$ W it is assumed that $\dot{Q}_H = 0$ W. In conclusion, $\dot{Q}_H = f(P_{in})$ is noncontinuous piecewise affine over a disjoint domain, i.e.

$$\dot{Q}_H = \begin{cases} \text{undefined} & \text{when } P_{in} < 0 \\ 0 & \text{when } P_{in} = 0 \\ \text{undefined} & \text{when } 0 < P_{in} < 700 \\ 3.404 P_{in} + 1380.4W & \text{when } 700 \leq P_{in} \leq 3500 \\ \text{undefined} & \text{when } P_{in} > 3500 \end{cases} \tag{3.4}$$

Since $\dot{Q}_H = f(P_{in})$ is nonlinear, the heat pump cannot be modelled as a linear model (i.e., the form in Equation 2.11 cannot be used). Also, since $m$ is positive, the COP is higher for lower input powers and decreases as the input power increases. See Figure 3.5.

### Constant COP

For the purpose of making a model with constant COP (such that the model is linear), the data is also fitted to a model $\dot{Q}_H = COP_{const} \cdot P_{in}$. Using the least squares method returns $COP_{const} = 4.5195$.

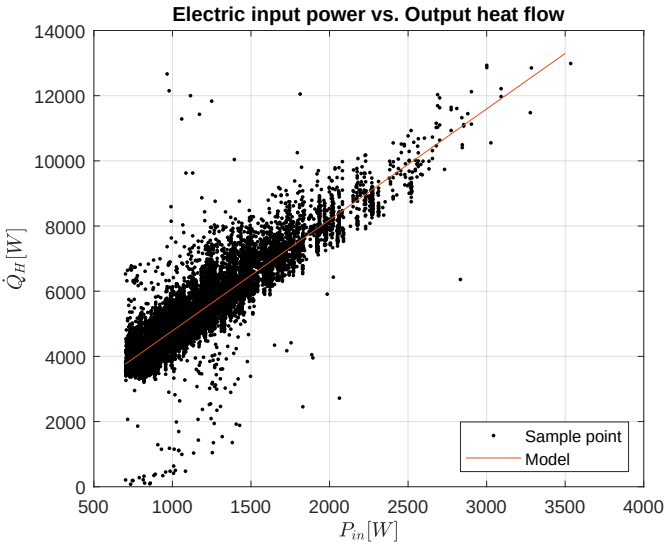


***Figure 3.4:*** *$n = 18275$ samples to which a model is fitted with linear regression. The model is $\dot{Q}_H = 3.404P_{in} + 1380.4\,[W]$ for $P_{in} \in [700, 3500]$ W. Evidently, there are some samples with values which deviate significantly from the model. Those are however few compared to the total amount of samples.*

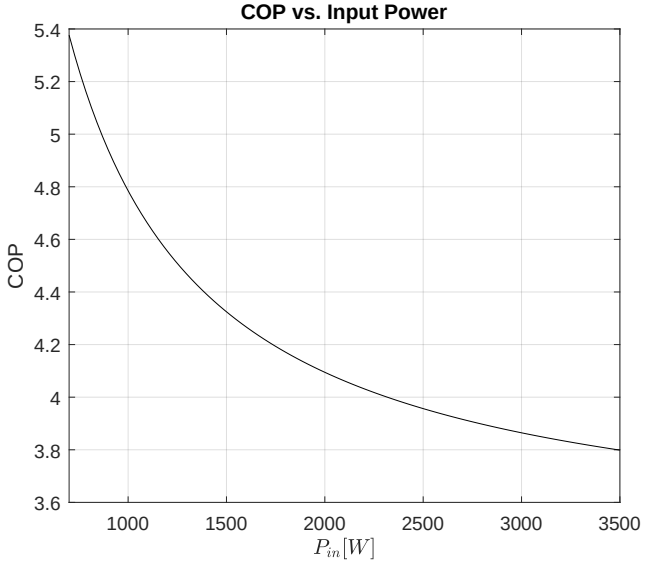


***Figure 3.5:*** *COP at varying input powers for the identified model.*

## 3.5 Controller

In this section, the implementation of two different controllers is described. The heat pump controllers used are a standard controller, which uses a heat curve to find the appropriate heat input to the house, and an MPC controller which uses weather forecasts and future electricity prices to optimize comfort and electricity cost based on a weight parameter.

### 3.5.1 Heat Curve Controller

The heat curve controller is used to enable comparisons between a standard heat pump controller and the developed MPC controller. Normally, the supply water temperature is a function of outside temperature. Since the supply flow rate is constant and the indoor temperature is relatively constant, the heat flow from the heat pump to the house can be assumed to be a function of the supply water temperature. Therefore, the standard way of implementing a heat curve controller is analogue to determining input power as a function of outside temperature. In this implementation, the water temperature is not modeled. Instead, the heat transfer from the heat pump to the house is determined directly as a function of outside temperature.

For a regular heat pump there are several heat curves to choose from. The choice of heat curve is made based on the need of the house. The heat curves can also be offset depending on desired reference indoor temperature. The reference indoor temperature is in this thesis chosen to be 21°C, meaning that only one heat curve is needed for the modeled house.

Calculating the heat curve for the linear state-space model of the house is done by finding the power demand, $\dot{Q}_H$, that satisfies a steady state indoor temperature equal to the reference temperature. Assuming zero solar radiation, steady state indoor temperature in Equation (3.1) and (3.2) gives

$$\dot{Q}_H = \frac{T_{in} - T_{out}}{R_{house}} \tag{3.5}$$

where $R_{house} = 5.3 \cdot 10^{-3}$°C/$W$ is the total thermal resistance of the house.

The heat curve is described by the equation

$$\dot{Q}_{H,demand} = kT_{out} + m \tag{3.6}$$

With a linear fit of the values $T_{in} = 21$°C, $T_{out} = [-21, 21]$°C the coefficients of the heat curve is calculated to be $[k, m] = [-188.6792, 3962.3]$, see Figure 3.6.

Heat pumps are generally not run on less than about 20% of their maximum input power. Instead, if the heat flow demand corresponds to an input power which is less than 20% of the maximum input power, the heat pump is run in bursts on its lowest input power. The lowest input power ($u = 700W$) corresponds to an output heat flow of 3.7635 kW. There will be one burst every hour since weather data (and thus heat flow demand) is only changing once every hour.

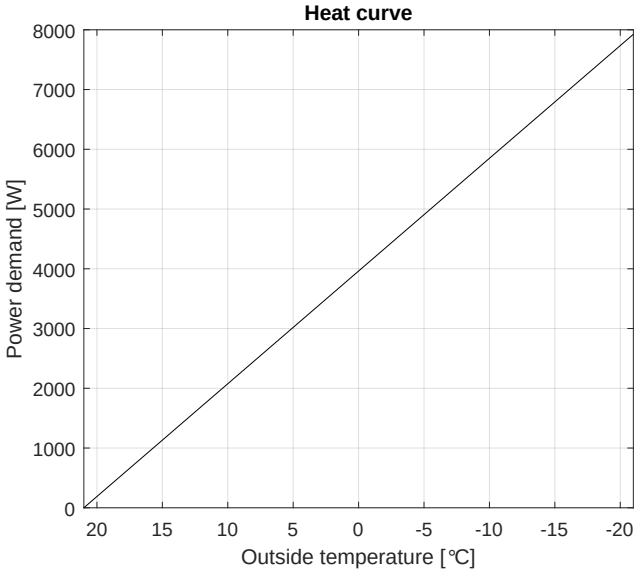


***Figure 3.6:*** *Theoretical heat curve ranging from −21°C to 21°C fully covering the temperature span used in this thesis. Temperatures are shown as decreasing according to industry standard.*

The length of the bursts will vary between 0 and 60 minutes and for the remainder of the hour the heat pump will be turned off. Given a certain heat flow demand ($\dot{Q}_{H,demand}$), the theoretical electric power demand ($\dot{Q}_{elec,theoretical}$) is calculated by dividing the heat flow demand with the COP at $u = 700W$. The length of the bursts (in seconds) are calculated according to Equation (3.7). For the duration of one hour this will provide an equal amount of heat transferred into the house system as if the heat pump would run constantly at a lower rate.

$$\text{Burst time} = 3600 \cdot \frac{\dot{Q}_{elec,theoretical}}{\dot{Q}_{elec,min}} \tag{3.7}$$

In real-world applications, the heat curve may be adjusted manually to match the specific house that the heat pump is used for. A simulation with real-world weather data is conducted to evaluate and shift the heat curve to match the power demand of the house. The evaluation is done for the whole period of acquired forecast data. See Figure 3.7.

Figure 3.7 shows a steady increase in indoor temperature as time progresses in the period. For this reason, the heat curve is adjusted with resulting coefficients $[k, m] = [-188.6792, 3652.3]$, giving indoor temperatures seen in Figure 3.8. The resulting heat curve is shown in Figure 3.9 and the burst time in Figure 3.10.

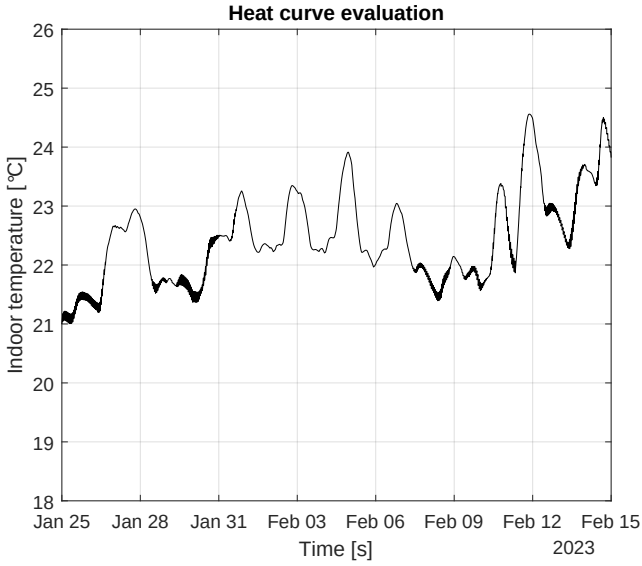


***Figure 3.7:*** *Evaluation of the theoretical heat curve neglecting disturbances due to solar radiation.*

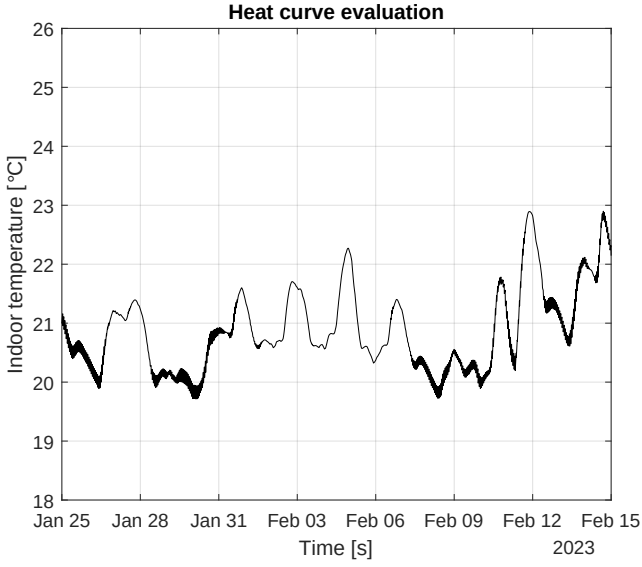


***Figure 3.8:*** *Evaluation of the heat curve after adjustment due to the disturbance of solar radiation.*

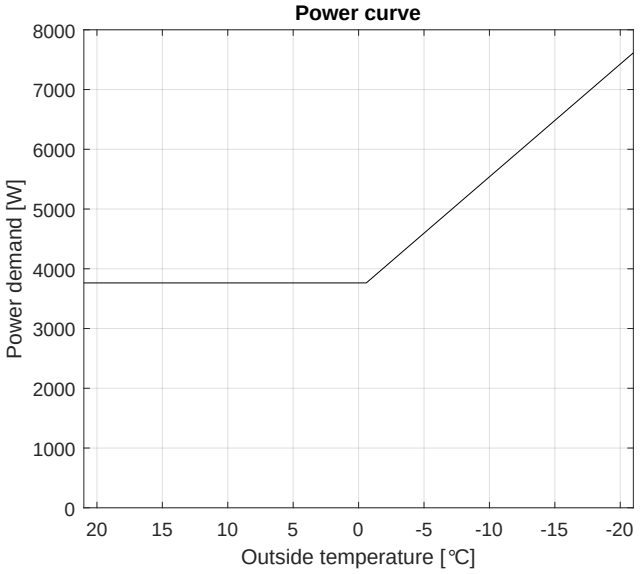


***Figure 3.9:*** *The heat curve after adjustment due to disturbances and with regards to the minimal operating input power.*

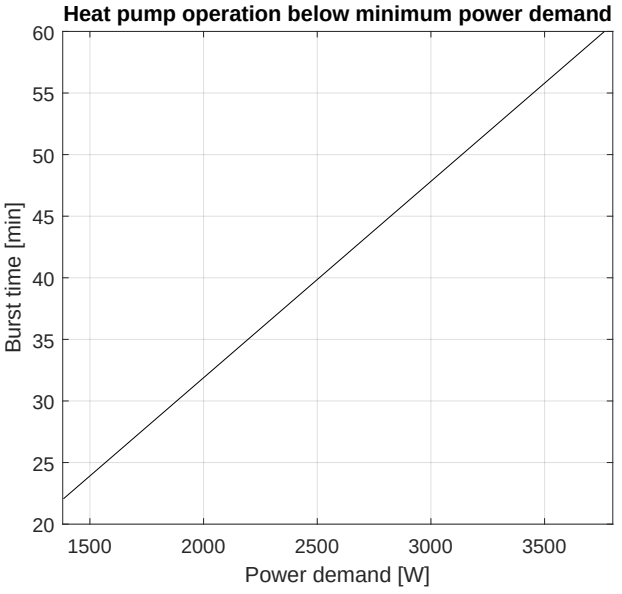


***Figure 3.10:*** *Burst time calculated for heat pump operating levels below the minimum threshold.*

### 3.5.2 MPC Controller

To utilize an MPC controller, a few different components are used. Practically, the controller is implemented in MATLAB with the optimization toolbox YALMIP [21]. This enables the usage of Simulink for the simulations. A simplified house model is developed to be used as the internal plant for the MPC controller. MATLAB is used for data handling as well as setting up the optimization objects in YALMIP for use in the MPC controller.

#### Dynamic model - RC modeling

The MPC requires a dynamic model representation of the system that is controlled. RC modeling is used in the same way as in Section 3.3. For this model, the solar radiation will be neglected since there is no forecast data which could be used when simulating. Attempts to use cloudiness forecast data to model solar radiation forecasts were conducted, but the correlation did not prove strong enough to be usable, see Appendix B. Thus there is no need to have a second degree model and hence a first degree model is used. Temperature, however, is of course included in the weather forecast. The RC model is shown in Figure 3.11.

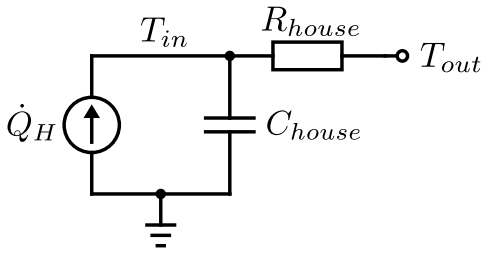


***Figure 3.11:*** *The one state RC-model which is used in the standard, constant COP, and perfect prediction MPC controllers.*

The values used for resistance and capacitance is the same as for the house model, $R_{house} = 5.3 \cdot 10^{-3}$ °C/W and $C_{house} = 24.5 \cdot 10^{6}$ J/°C.

#### State-space MPC model

From the RC-model in Figure 3.11 a state-space model with one state, indoor temperature ($T_{in}$), is derived. $T_{in}$ is measured. The controlled input signal is the heating power ($\dot{Q}_H$) and one measured disturbance, outside temperature ($T_{out}$), is affecting the house. The model is described by the differential equation

$$\dot{T}_{in} = \frac{1}{C_{house}R_{house}}(T_{out} - T_{in}) + \frac{1}{C_{house}}\dot{Q}_H \tag{3.8}$$

which is rewritten on state-space form

$$\dot{x} = Ax + Bu + Ew$$
$$y = Cx + Du$$

where

$$x = T_{in}, \quad u = \dot{Q}_H, \quad w = T_{out}$$
$$A = -\frac{1}{C_{house}R_{house}}, \quad B = \frac{1}{C_{house}}, \quad E = \frac{1}{C_{house}R_{house}}$$
$$C = 1, \quad D = 0$$

### Discretized model

The internal model used in the controller is discretized in time steps equal to the sample time of the controller, $T_s$. The discretization is done in MATLAB using the zero-order hold (ZOH) method. The resulting discretized model is written on the form in Equation (2.11) where

$$A_d = 0.9954, \quad B_d = 2.4433 \cdot 10^{-5}, \quad E_d = 0.00461$$
$$C_d = 1, \quad D_d = 0$$

### Controller layout

The controller uses a sample time of 10 minutes. This sample time was chosen for a few different reasons. For one, 10 minutes is a reasonable operational cycle time for the compressor. NIBE prefers to run the compressor for at least 5 minutes when it is turned on, and let it stay turned off for 5 minutes when it is turned off. In general it is advantageous to run the compressor for fewer but longer periods since it is worn every time it is started up. Thus, having fewer start ups per day will prolong its lifespan. The response of a step input to the house model has a time constant of about 130 000 seconds which is about 217 sample times. For this reason, the sample time could be longer but is kept to 10 minutes due to the mentioned reasons. Apart from the current state, the controller also takes weather forecasts, and spot prices as inputs, see Equation (3.9). In this thesis spot prices are assumed to be available at 12:00 immediately as the bidding on the day-ahead market Elspot has ended, this is possible because of the use of historic data, since they are not released at exactly the same time every day. With this assumption, spot prices are available between 12 and 36 hours in advance and depending on the time of day, the prediction horizon will change (see Figure 3.12). The spot price, provided in SEK/MWh, is converted to SEK/J as it is to be multiplied with the time step duration (in seconds) and the control signal which is in watts (J/s). Thus it is preferable to use SI-units to the furthest extent possible.

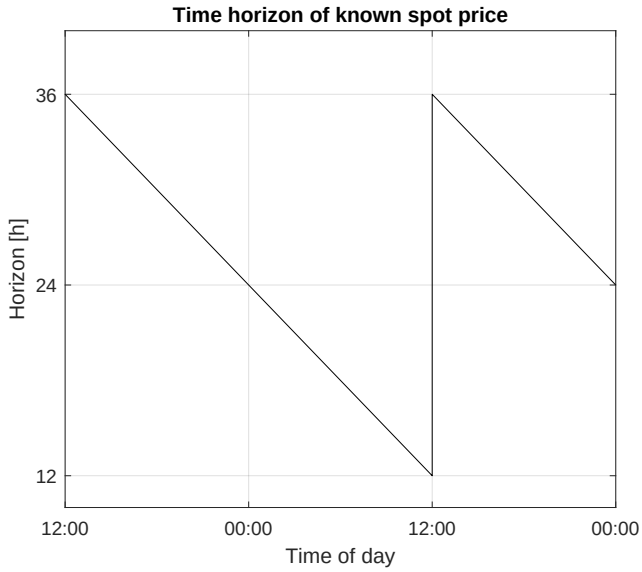


***Figure 3.12:*** *At 12:00 CET each day the next days hourly spot prices collected creating a horizon of 12-36 hours ahead with known prices.*

Weather forecasts are always available further in advance than spot prices, and thus it is the spot price horizon that limits the controller horizon. Due to this, the controller must be able to handle a dynamically shifting horizon. With spot prices available from 12:00 CET, the maximum control horizon will be used at 12:00 CET, which will be $N = 216$ (36 hours $\cdot$ 6 samples/hour = 216 samples). The control horizon will then decrease by one at each time step, until it reaches $N = 73$ at 11:50 CET the next day (12 hours $\cdot$ 6 samples/hour + 1 sample = 73 samples).

### Soft constraint

In order to limit the indoor temperature from deviating too much from the reference temperature without increasing the cost/comfort-weight ($\alpha$), a soft constraint on the difference between indoor- and reference indoor temperature is implemented. The comfort range is chosen to be $\pm 2$°C. A constraint containing the slack variable $\epsilon$ is used such that if the temperature deviates less than or equal to 2°C it does not add to the objective function as $\epsilon$ is equal to zero. As the temperature deviates more than 2°C, $\epsilon$ will be non-zero which introduces an increase of the objective value. $\epsilon$ is multiplied by a penalty factor $R_\epsilon$ to scale the resulting penalty to have a large effect. $R_\epsilon$ is chosen to be $10^5$. The penalty of deviating more than 2°C is designed to be linear meaning that each degree outside of the comfort range of 2°C adds an equal amount to the total objective value. The penalty for deviating is chosen large enough in this context such that

breaking the soft constraint will never be worth it in practical use, i.e., for reasonable electricity cost and weather conditions. Using a soft constraint instead of a hard constraint will however make sure that the problem is solvable even if the temperature for some reason has fallen under or risen above the desired levels.

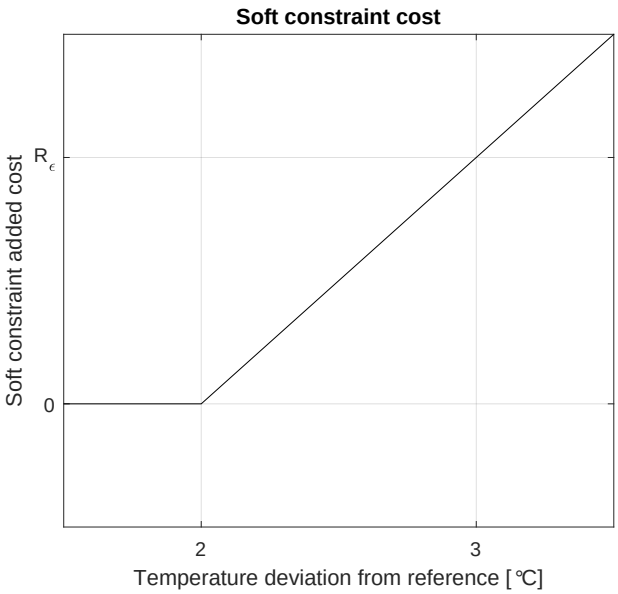


***Figure 3.13:*** *Illustration of the objective function penalty for deviating from the comfort temperature range.*

### Control problem

The mathematical description of the control problem is

$$
\begin{aligned}
\min_{u} \quad & \sum_{j=0}^{N-1} \alpha |y_{k+j|k} - r| + \alpha \epsilon R_\epsilon + (1-\alpha) c_e T_s u_{k+j|k} \\
\text{s.t.} \quad & u_{k+j|k} \in \{0, [700, 3500]\} \quad \forall j = 0, ..., N-1 \\
& |y_{k+j|k} - r| - \epsilon \leq 2 \quad \forall j = 0, ..., N-1 \\
& y_{k+j|k} = C x_{k+j|k} \quad \forall j = 0, ..., N-1 \\
& x_{k+j+1|k} = A_d x_{k+j|k} + B_d f(u_{k+j|k}) + E_d w_{k+j|k} \quad \forall j = 0, ..., N-1
\end{aligned}
\tag{3.9}
$$

where

$$\begin{aligned} r \in \mathbb{R}\ [^\circ C] &: \text{reference indoor temperature} \\ u \in \mathbb{R}\ [W] &: \text{input power} \\ w\ [^\circ C] &: \text{outside temperature forecast} \\ c_e\ [SEK/J] &: \text{electricity cost} \\ T_s\ [s] &: \text{sampling time} \\ 0 < \alpha \leq 1 &: \text{cost/comfort-weight} \\ 0 \leq \epsilon &: \text{soft constraint slack variable} \end{aligned}$$

#### Implementation in YALMIP

In the implementation, the objective function in Equation (3.9) is rescaled

$$\sum_{j=0}^{N-1} |y_{k+j|k} - r| + \epsilon R_\epsilon + \frac{1-\alpha}{\alpha} c_e T_s u_{k+j|k} = \sum_{j=0}^{N-1} |y_{k+j|k} - r| + \epsilon R_\epsilon + \beta u_{k+j|k} \quad (3.10)$$

where

$$\beta = \frac{1-\alpha}{\alpha} c_e T_s \quad (3.11)$$

$\beta$ is evaluated before calling the optimizer. This is done to reduce the amount of parameters in the model, which will lead to better optimization performance. While the objective functions are not equal, they are equivalent with respect to their optimal parameters, as Equation (3.9) has been divided by $\alpha$ which is a positive constant during each run.

In the YALMIP implementation, the controller is parameterized in the model states ($x$), reference ($r$), input ($u$), disturbances ($w$), and $\beta$. The initial state, reference, disturbances, and $\beta$ are constrained when the optimizer is called, while each state starting from the second is constrained so that it satisfies the dynamic equation. An optimizer object is defined for each possible control horizon. This means that a total of 144 optimizer objects are defined (individual horizons = maximum horizon - minimum horizon + 1 = 216 − 73 + 1 = 144). At each call, the optimizer object which corresponds to the current horizon is called.

The problem is nonlinear due to the nonlinear COP function, and since $u$ is a semi-continuous variable. This means that the optimization problem cannot be solved by common LP solvers. It can however be solved with a *Mixed Integer Linear Programming* (MILP) solver. A MILP solver supports the integer programming introduced by the constraints on $u$, and does also support the use of the piecewise affine COP function. Gurobi is used in this thesis. For performance reasons, an optimal solution is deemed to be found when the gap between the current best solution and the lower bound goes below $10^{-3}$. Therefore the solutions will not be optimal, but this simplification is necessary to make in order for the problem to be solvable in a reasonable time.

## 3.6 Weather Prediction

Once every hour, SMHI releases a weather forecast for the next 10 days. These forecasts were sampled between 2023-01-25 and 2023-02-16. For the first 44 - 48 hours of a forecast there are values for each hour, meaning that there exist forecasts for every hour of the 36 hour horizon dictated by the spot price. Values for temperature are taken directly from the forecast and used in the simulation. As no value for radiation is given in the forecast, a model was created which returns radiation as a function of known parameters. Cloudiness and sunshine is included in SMHI-supplied forecasts and was used when modelling solar radiation. The correlation to observed solar radiation values turned out too weak to be used. Solar radiation was thus not used in the weather forecast. For details on the model, see Appendix B.

### 3.6.1 Temperature Forecast Quality

The quality of the forecasts is analysed by comparing the predicted temperatures with observations. Hourly forecasts in the period 24 January 2023 23:00 CET to 13 February 2023 23:00 CET are analysed. For each forecast, the first 48 hours are evaluated against the corresponding observations. This means that the period for which forecasts are compared with measured values is 25 January 00:00 CET to 15 February 23:00 CET. For each forecast horizon, the average deviation from the observed temperature is calculated. Figure 3.14a shows the mean error for each specific horizon as well as the interval for one standard deviation. Figure 3.14b shows the standard deviation from the observed value for each specific horizon.

As expected, the standard deviation is the smallest for the shortest forecast horizon and increases for longer horizons. For this data, the deviation increases until around a 10 hour horizon, after which it stays around the same until 30 hours. After around 35 hours, the standard deviation starts to rise rapidly. It should be noted that the horizon used in the controller will be at most 36 hours. Therefore, the standard deviation is at most around 1.85°C in this implementation.

#### Missing weather forecasts

Some forecasts are missing due to errors during sampling. Figure 3.15 shows the amount of missing forecasts per day (a day without missing forecasts should have 24 forecasts, one for each hour). Evidently, the amount of missing forecasts is very high during the end of the period. To solve this problem, previous forecasts are used when data is lacking for a specific hour. The previous forecast is shifted one hour in time to act as a replacement.

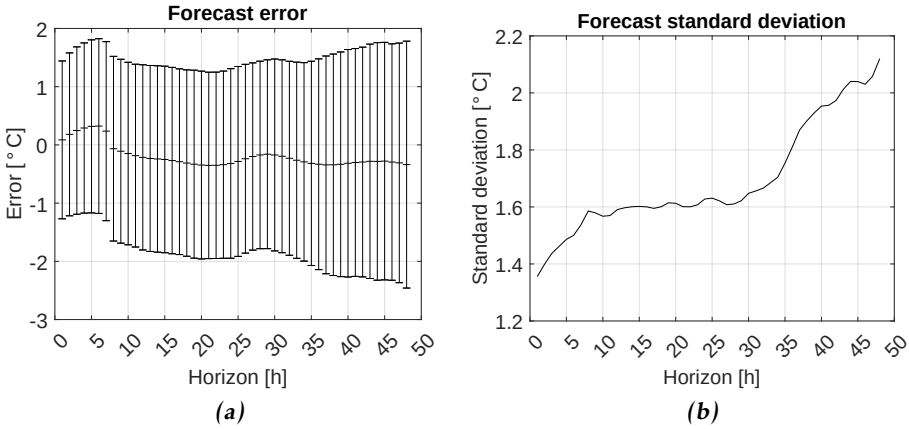


***Figure 3.14:*** *Mean forecast error per horizon and the standard deviation from observed values.*

Using old forecasts may decrease accuracy. To evaluate the quality of each forecast, the mean standard deviation from observed temperatures for all horizons is evaluated for each forecast. The standard deviation from observed temperature is shown in Figure 3.16. It is clear that the deviation is higher during the end of the period (around February 9 to 14) when there are more missing forecasts.

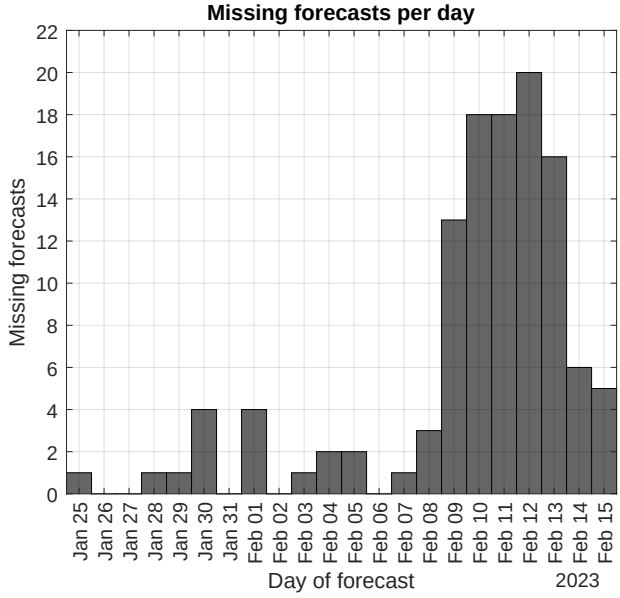


***Figure 3.15:*** *Amount of missing forecasts per day.*

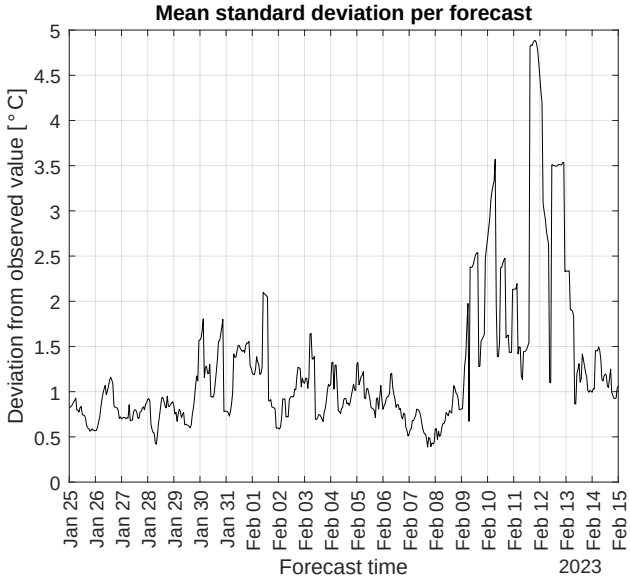


***Figure 3.16:*** *Mean standard deviation between forecasts and observed temperature for all horizons.*

# 4

# Benchmarking and Results

The controllers are evaluated using three different cases where each case contains weather and spot price data for one week. The three weeks are simulated separately using the controllers to control the indoor temperature. MATLAB and Simulink are used to implement the models and run the simulations with acquired weather and spot price data. The simulations are benchmarked using two measurements, electricity cost and degree minutes. The results come in the form of data extracted from the simulations in Simulink. Regarded as performance is what corresponds to the overall aim of minimizing electricity cost while maintaining comfort (degree minutes). The data presented would be of direct interest for a user. The second part of the results is the control of the heat pump in the form of control signal distribution which shows how the heat pump is operated during the three periods.

## 4.1 Analysed Cases

The cases which are analysed are limited in time to the sampled weather forecast data. This period does however provide a range of different operating conditions which was analysed. During the period, the spot price varied between 0.02 SEK/kWh and 2.44 SEK/kWh, see Figure 4.1.

The cases which are possible to analyse are limited to the conditions during the recorded period. Therefore, the studied cases do not necessarily cover all interesting conditions. However, the period contains varying conditions which are typical during the winter season in southern Scandinavia. As this is the season with the lowest temperature, the heating demand is the highest and thus the potential savings are also the highest.

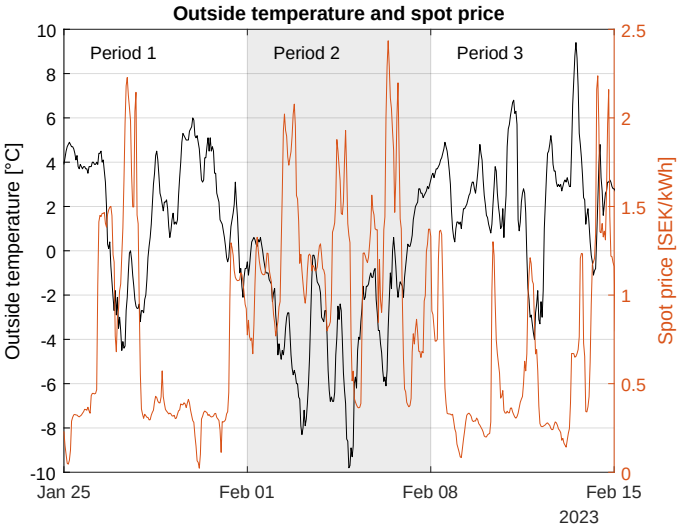


***Figure 4.1:*** *Outside temperature in Norrköping and spot price during the whole period when forecasts were sampled. There is a negative correlation of -0.48 between outside temperature and spot price.*

### 4.1.1 Period 1: 7 Days with Highly Varying Spot Prices

The first period mostly includes outside temperatures of around 0 to 6 °C and around 1.5 days with temperatures below 0 °C. The temperature and spot price are inversely correlated (the correlation coefficient is -0.55), see Figure 4.2. This is the biggest inverse correlation of the analysed periods.

### 4.1.2 Period 2: 7 Days with High Spot Prices and Cold Weather

During most of period 2 the outside temperature was below 0 °C. The spot price is very cyclic with high prices during the day and lower during the nights (with clear peaks during morning and afternoon for all days). The correlation coefficient between temperature and spot price is -0.18, see Figure 4.3.

### 4.1.3 Period 3: 7 Days with Low Spot Prices, Warm Weather and High Prediction Errors

Period 3 shows significant differences during the period for both temperature and spot price. The correlation between temperature and spot price is -0.14, see Figure 4.4. Note that this period has significantly larger errors in its forecasts compared with period 1 and 2, see Figure 3.16. This provides an opportunity to study the effects of prediction errors.

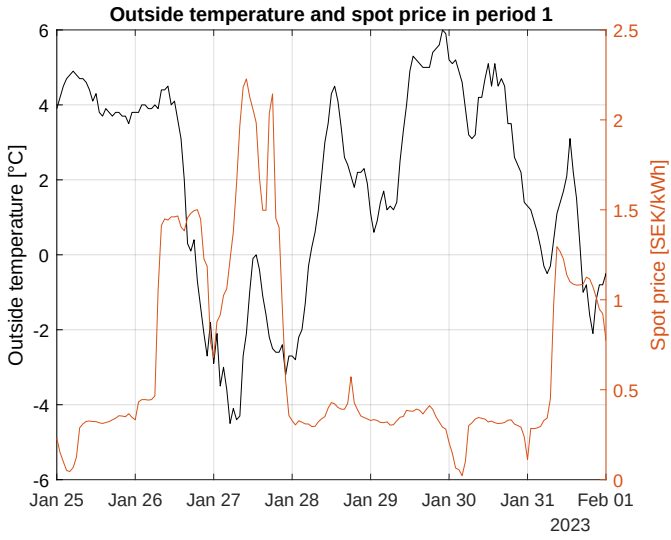


***Figure 4.2:*** *Outside temperature in Norrköping and electricity spot price during period 1.*

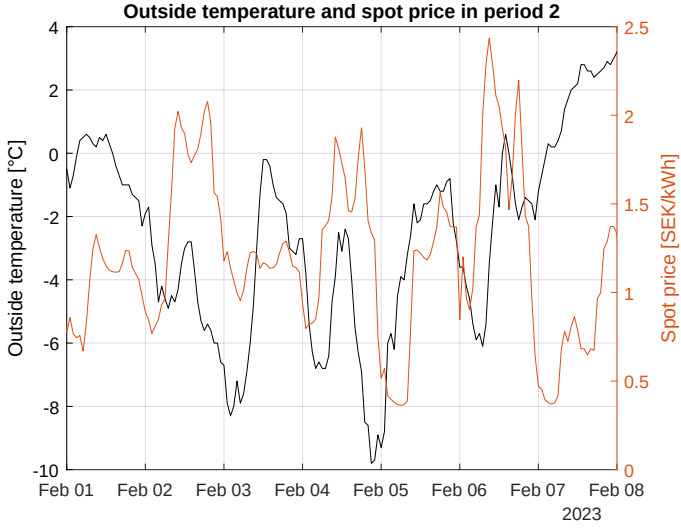


***Figure 4.3:*** *Outside temperature in Norrköping and electricity spot price during period 2.*

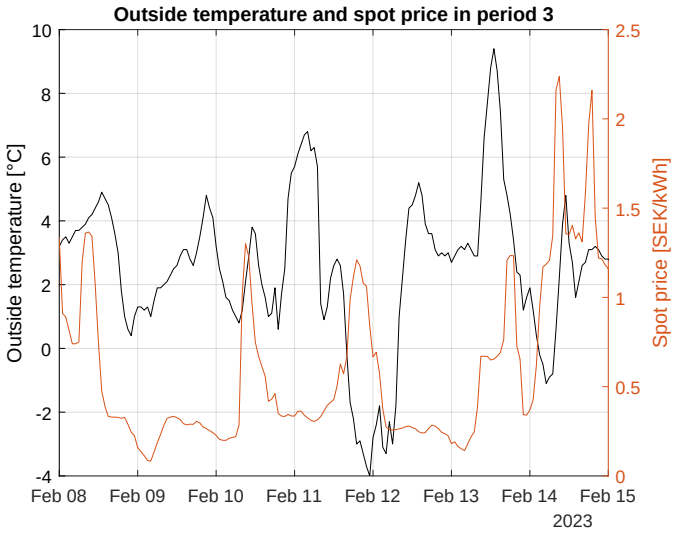


***Figure 4.4:*** *Outside temperature in Norrköping and electricity spot price during period 3.*

## 4.2 Benchmarking

The developed MPC controller, referred to as the *standard* MPC Controller, is compared with four other controllers. Three of those are variations of the standard MPC controller, while the fourth is the heat curve controller.

- **Constant COP MPC controller.** If COP is a constant value, the entire system is a Linear Time Invariant (LTI) system. This leads to a simpler optimization problem which is significantly faster to solve. It is therefore interesting to study whether it is possible to use a constant COP in the controller model while using the more realistic, varying COP in the simulated heat pump model.
- **Perfect prediction MPC controller.** This controller is equal to the standard MPC controller in all aspects except that it is fed with predictions which are made from observation data, meaning that the predictions will always be exactly correct. This controller is used for the purpose of evaluating the effects of prediction errors on controller performance.
- **Oracle MPC controller.** This controller is an MPC controller which uses the second order model from Section 3.3 as dynamic model in the controller with perfect predictions for all disturbances, including radiation. $C$ is in this case $[1, 0]$ The controller thus has a perfect understanding of the how the system will behave during the horizon. Comparing the performance of this controller to the perfect prediction MPC gives a measurement of how the model errors affect performance.

- **Heat curve controller.** This is the standard heat curve controller described in Section 3.5.1. It is used as a baseline to compare the performance of the MPC controller.

The controllers are evaluated in electricity cost and comfort. The cost evaluation is fairly simple and intuitive. In simulation, the current spot price is multiplied with the current input power and integrated over time, giving the total electricity cost during one simulated period. The cost is then compared between the controllers. The comfort evaluation is somewhat less intuitive. The method used here is called *degree minutes* [22], which is a way of measuring deviation from reference temperature. 1 degree minute corresponds to a deviation from the reference temperature of 1 degree for 1 minute. Mathematically, degree minutes can be defined

$$\text{degree minutes} = \int_{t_0}^{t_1} |T_{in}(t) - r(t)| dt$$

where $t$ is measured in minutes. It should be noted that this is the same way of quantifying comfort as is done in the objective function. Never deviating from the reference temperature will result in 0 degree minutes and staying on the comfort range boundary (±2°C) for a whole period of 7 days results in 20160 degree minutes.

The MPC controllers are evaluated for different values of $\alpha$ and the heat curve controller is evaluated for its calibrated setting.

## 4.3 Performance

For all periods, degree minutes and total electricity cost is presented in tables for all controllers. Indoor temperature is plotted against spot price for the standard MPC using $\alpha = 0.010$ in this chapter. For plots of the performance of all controllers, refer to Appendix A. The values for $\alpha$ during simulations were chosen to be $\alpha_1 = 0.005$, $\alpha_2 = 0.010$, and $\alpha_3 = 0.015$. For the standard MPC, $\alpha_4 = 1$ was also included. The MPC controller uses a time step of 10 minutes giving a 10 minute linear indoor temperature behaviour. The heat curve controller was simulated using the controller developed in Section 3.5.1. All simulations were conducted using a constant reference temperature ($r$) of 21°C.

### 4.3.1 Period 1

Period 1 ranges from Jan 25 to Feb 1 of the year 2023. Indoor temperature and spot price during the period is shown in Figure 4.5 where $\alpha = 0.010$. Accumulated degree minutes and total electricity cost for different values on $\alpha$ for all controllers are shown in Table 4.1.

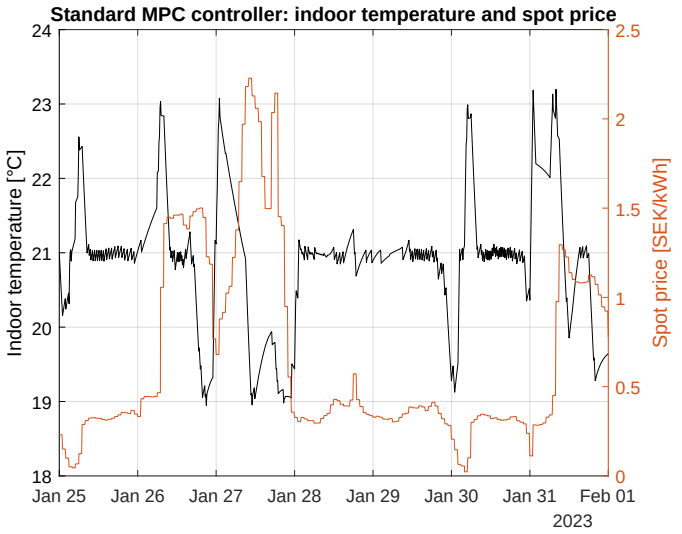


***Figure 4.5:*** *Simulation during period 1 from Jan 25 to Feb 1. Standard MPC controlled indoor temperature with $\alpha = 0.010$ on the left axis and spot price on the right axis.*

***Table 4.1:*** *Comfort and electricity cost results from simulations of period 1, Jan 25 to Feb 1.*

| Controller | $\alpha$ | Degree minutes [°C min] | Cost [SEK] |
|---|---|---|---|
| Standard MPC | 0.005 | 8761 | 61.41 |
| —"— | 0.010 | 5624 | 62.94 |
| —"— | 0.015 | 3482 | 65.94 |
| —"— | 1 | 443 | 91.04 |
| Constant COP MPC | 0.005 | 9295 | 70.79 |
| —"— | 0.010 | 6960 | 74.37 |
| —"— | 0.015 | 4995 | 77.09 |
| Perfect prediction MPC | 0.005 | 8707 | 61.11 |
| —"— | 0.010 | 5517 | 63.30 |
| —"— | 0.015 | 3436 | 66.27 |
| Oracle controller | 0.005 | 7719 | 60.63 |
| —"— | 0.010 | 3806 | 64.64 |
| —"— | 0.015 | 2694 | 66.28 |
| Heat curve controller | N/A | 8018 | 77.73 |

### 4.3.2 Period 2

Period 2 ranges from Feb 1 to Feb 8 of the year 2023. Indoor temperature and spot price during the period is shown in Figure 4.6 where $\alpha = 0.010$. Accumu-

lated degree minutes and total electricity cost for different values on $\alpha$ for all controllers are shown in Table 4.2.

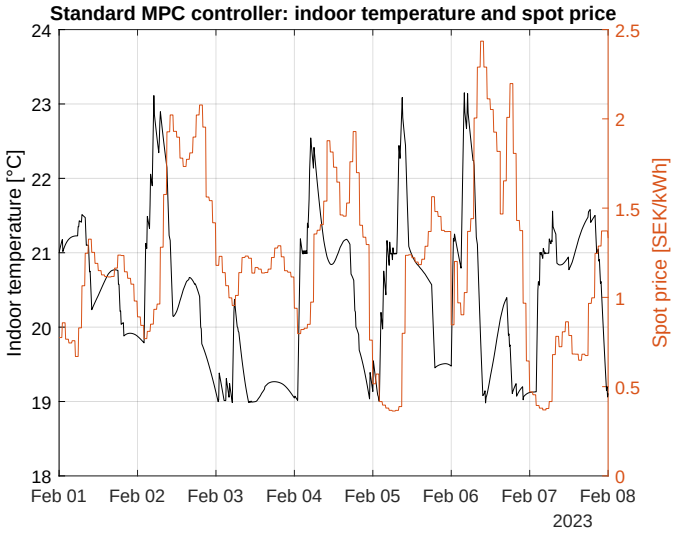


***Figure 4.6:*** *Simulation during period 2 from Feb 1 to Feb 8. Standard MPC controlled indoor temperature with $\alpha = 0.010$ on the left axis and spot price on the right axis.*

***Table 4.2:*** *Comfort and electricity cost results from simulations of period 2, Feb 1 to Feb 8.*

| Controller | $\alpha$ | Degree minutes [°C min] | Cost [SEK] |
|---|---|---|---|
| Standard MPC | 0.005 | 11911 | 143.16 |
| —"— | 0.010 | 9403 | 144.62 |
| —"— | 0.015 | 6455 | 148.17 |
| —"— | 1 | 287 | 179.55 |
| Constant COP MPC | 0.005 | 13144 | 162.56 |
| —"— | 0.010 | 10593 | 169.52 |
| —"— | 0.015 | 8992 | 173.84 |
| Perfect prediction MPC | 0.005 | 11741 | 143.90 |
| —"— | 0.010 | 8659 | 145.45 |
| —"— | 0.015 | 6553 | 148.17 |
| Oracle controller | 0.005 | 12131 | 141.22 |
| —"— | 0.010 | 8814 | 143.86 |
| —"— | 0.015 | 4717 | 149.83 |
| Heat curve controller | N/A | 4106 | 167.34 |

### 4.3.3 Period 3

Period 3 ranges from Feb 8 to Feb 15 of the year 2023. Indoor temperature and spot price during the period is shown in Figure 4.7 where $\alpha = 0.010$. Accumulated degree minutes and total electricity cost for different values on $\alpha$ for all controllers are shown in Table 4.3.

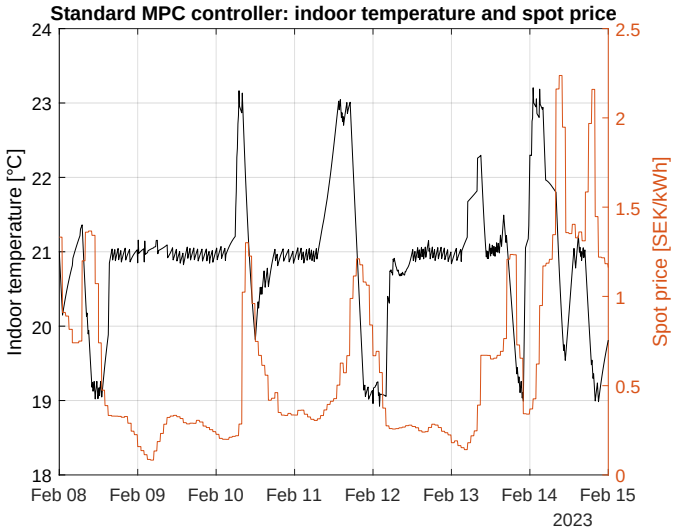


***Figure 4.7:*** *Simulation during period 3 from Feb 8 to Feb 17. Standard MPC controlled indoor temperature with $\alpha = 0.010$ on the left axis and spot price on the right axis.*

***Table 4.3:*** *Comfort and electricity cost results from simulations of period 3, Feb 8 to Feb 15.*

| Controller | $\alpha$ | Degree minutes [°C min] | Cost [SEK] |
|---|---|---|---|
| Standard MPC | 0.005 | 9471 | 42.98 |
| —"— | 0.010 | 5844 | 45.55 |
| —"— | 0.015 | 5069 | 46.19 |
| —"— | 1 | 401 | 68.60 |
| Constant COP MPC | 0.005 | 10213 | 51.35 |
| —"— | 0.010 | 6874 | 54.25 |
| —"— | 0.015 | 5247 | 55.35 |
| Perfect prediction MPC | 0.005 | 9538 | 43.15 |
| —"— | 0.010 | 5958 | 45.33 |
| —"— | 0.015 | 5035 | 46.31 |
| Oracle controller | 0.005 | 6857 | 43.48 |
| —"— | 0.010 | 4580 | 45.73 |
| —"— | 0.015 | 3394 | 47.71 |
| Heat curve controller | N/A | 12552 | 65.86 |

## 4.4 Control Signal Characteristics

Each time step the MPC generates a control signal $u$ which is constrained as $u \in \{0, [700, 3500]\}$. See Appendix A.13 for an example of how the input signal changes during one period.

For every controller, the operating time distribution is shown. *Operating time* refers to the time when $u \neq 0$. Control signal is presented for simulations done with the standard MPC for the three periods, see Figures 4.8, 4.9, and 4.10.

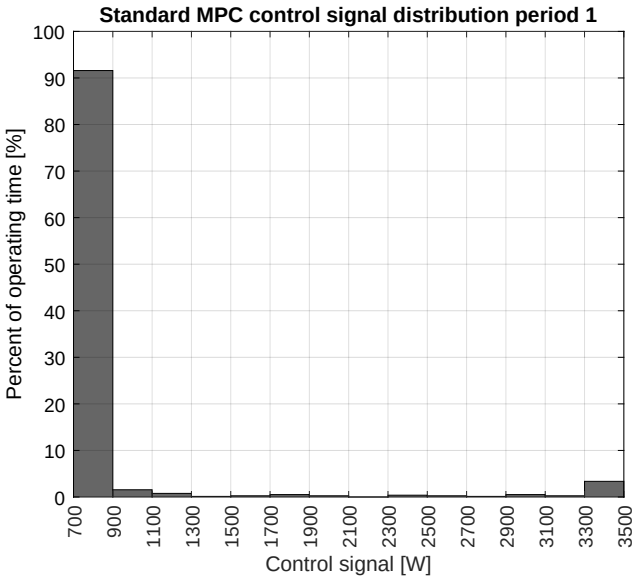


***Figure 4.8:*** *Distribution of the control signal during period 1 for the Standard MPC with* $\alpha = 0.010$*. The heat pump was operating (*$u \in [700, 3500]$*) for* 76.6% *of the total period and turned off (*$u = 0$*) for* 23.4%*.*

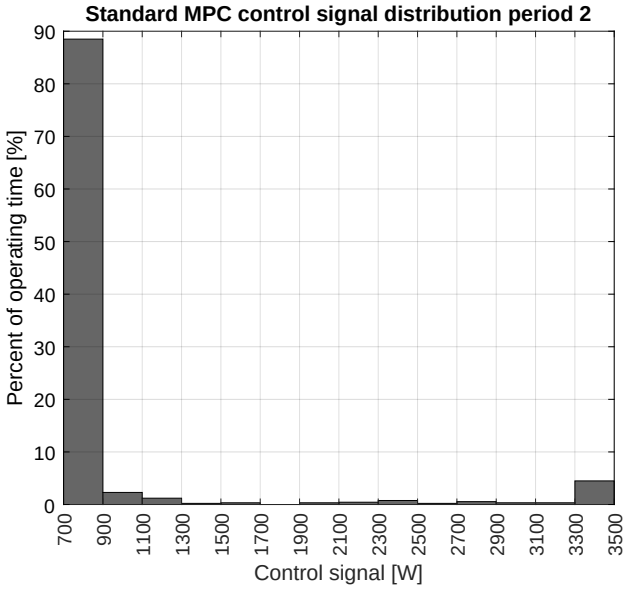


***Figure 4.9:*** *Distribution of the control signal during period 2 for the Standard MPC with* $\alpha = 0.010$*. The heat pump was operating (*$u \in [700, 3500]$*) for* 90.5% *of the total period and turned off (*$u = 0$*) for* 9.5%*.*

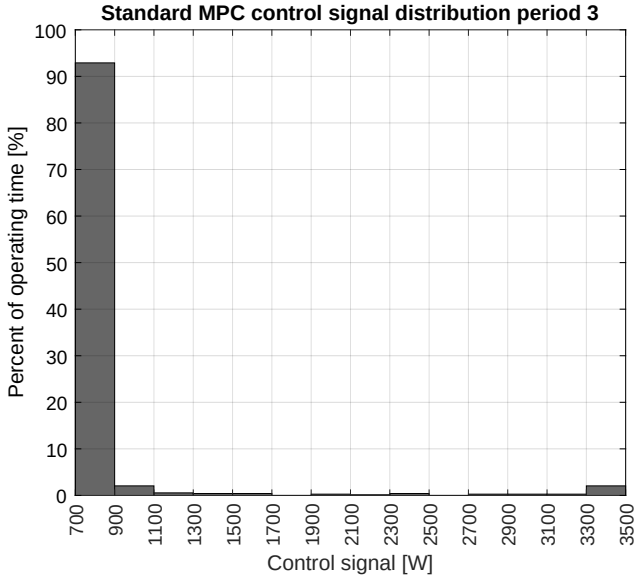


***Figure 4.10:*** *Distribution of the control signal during period 3 for the Standard MPC with* $\alpha = 0.010$*. The heat pump was operating (*$u \in [700, 3500]$*) for* 72.5% *of the total period and turned off (*$u = 0$*) for* 27.5%*.*

# 5

# Discussion and Conclusion

Multiple parts of the method and results gives reason for analysis. In this chapter, the benchmarking method and results are discussed with focus on controller comparison. System and model design regarding house and controllers including some problems that arises when designing models are explained. The MPC approach is considered for implementation in consumer products and some aspects of the feasibility of real-world implementation is discussed. A conclusion is drawn with the problem formulation, method, and results as foundation. Also some suggestions of future work is included.

## 5.1 Constant vs. Varying COP

In this thesis, using a constant COP was detrimental to controller performance. In some cases it could save money compared to the heat curve controller, but in the worst case (period 2, $\alpha = 0.015$) it provided lower comfort at a higher electricity cost when compared to the heat curve controller. It was always underperforming significantly compared to the standard MPC. It is therefore necessary to take the variations of COP into account when computing the cost which is very reasonable. By the nature of the problem at hand, power consumption is desired to be concentrated to the hours when the electricity is cheap. This will result in a more uneven power consumption when compared to traditional control methods. In other words, using a lot of energy at once or none at all is desired. On the other hand, COP is highest for low power inputs and lowest for high power inputs (see Figure 3.5). From a pure COP perspective, it would thus be most beneficial to use a low but steady power consumption. Evidently, there is a conflict of interest here which needs to be taken into account by the MPC. By taking both spot price and efficiency (COP) into account, the input power trajectory which yields the lowest total objective value can be calculated.

## 5.2 Sensitivity to Forecast Errors

The effects of weather forecast errors can be evaluated by comparing the standard MPC with the perfect prediction MPC. In this thesis, the effects are very small. On average for all $\alpha$, the standard controller had 69 degree minutes more compared to the perfect prediction controller in period 1, 272 more in period 2, and 40 less in period 3. The controllers were very similar in electricity cost during all three periods. On average for all $\alpha$, the standard MPC was 0.13 SEK cheaper during period 1, 0.54 SEK cheaper during period 2, and 0.02 SEK cheaper during period 3. Interestingly, the standard MPC was therefore both cheaper and provided better comfort during period 3, when the prediction errors were larger (see Figure 3.16). Overall, the errors are negligible. This might be due to radiation not being used in the MPC internal plant model. Variations in radiation would then have a larger effect than the prediction errors. Using publicly available weather forecasts (in this case from SMHI) should therefore work well for building climate control purposes.

## 5.3 Model Complexity

The oracle controller was used to evaluate whether the model simplifications would significantly reduce controller performance. The oracle controller is compared with the perfect prediction controller to remove the effects of prediction errors. Figure 5.1 visualizes degree minutes for both controllers for each case while Figure 5.2 visualizes electricity cost. In general, the oracle controller yields better comfort for very similar electricity cost as the perfect prediction controller. In fact, the electricity cost is often marginally higher for the oracle controller while the degree minutes are mostly significantly lower. It could thus be argued that the model simplifications primarily reduces comfort, while the differences in electricity cost are too small to be noteworthy. This means that if a good radiation model can be developed there is significant potential for improved comfort. A radiation model was planned to be used in this thesis, but could not be implemented in the end (see Appendix B).

Another consideration which should be taken into account before expanding the plant model to two states is how the second state should be estimated. The second state is the temperature in the middle of the walls, which may not be reasonable to measure. In reality, this temperature will probably be different in different places in the house. Probably, a better approach than measuring is to use an observer. The observer can for example be implemented using a Kalman filter [20] with the same two state model as is used in the controller.

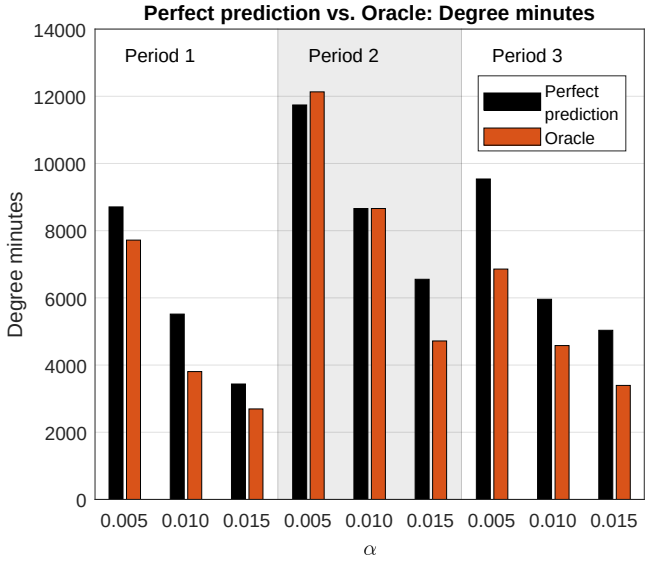


***Figure 5.1:*** *Deviation from reference temperature for the perfect prediction- and oracle controller for all periods and values of $\alpha$.*

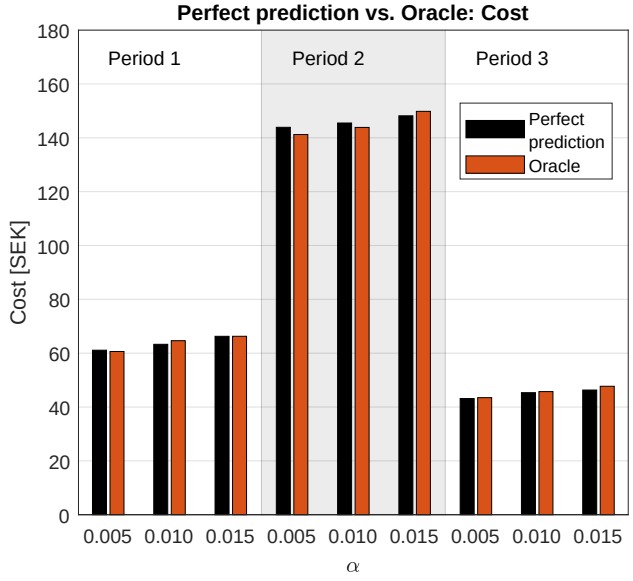


***Figure 5.2:*** *Electricity cost for the perfect prediction- and oracle controller for all periods and values of $\alpha$.*

## 5.4 Forecasting Radiation

Models for estimating global radiation based on sunshine and cloudiness respectively (as well as data for time of day and day of year) are presented in Appendix B. For the case that data for sunshine can be accessed, a good model of radiation is possible to make. The cloudiness model however is less robust and may sometimes over- or underestimate radiation significantly, especially during winter. As heating is needed the most during winter, it was decided to not include the radiation model in the prediction. It is however possible that the radiation model can provide improved performance, although this will need to be weighed against the increase in model complexity.

## 5.5 Overdimensioned Heating System

Identification of the COP model used in this thesis was done with a real world operating heat pump. The data available was for a house that uses a ground source heat pump with 18 kW capacity. There was not enough data in order to use the same house for the house modeling and thus data from another house had to be used. This led to an overdimensioned heat pump, i.e., higher power output capacity than needed, with regards to the house. Using Equation (3.5) to calculate the outside temperature necessary to run the heat pump on full capacity gives $-74.4°C$ and $1.1°C$ for the lowest capacity. A lower capacity heat pump would cover the outside temperature span used in the analysed cases. An 8kW heat pump would cover temperatures between $-21.4°C$ and $12.1°C$ without the need of the burst heating in the heat curve controller since it would never run on its lowest capacity.

The fact that the heat pump is often running on low power means that COP is most often very good. If a heating system of more suitable capacity was to be used, the heat pump would have to run at a higher percentage of its maximum power. The COP would then be somewhat lower.

## 5.6 Comfort vs. Cost

The trade off between comfort and cost is unavoidable when managing house heating. In this thesis there are some values that can be tuned. Weight ($\alpha$) and comfort temperature range are two parameters that is reasonable for a consumer to tune in order to meet the demands.

### 5.6.1 Weight

The weight ($\alpha$) is a tuning parameter and could in real applications be chosen by the consumer to have the MPC tuned to the users preference. Large $\alpha$ gives priority to maintaining comfort while a small $\alpha$ results in a bigger priority on saving money. It is possible to have $\alpha = 1$, however with our implementation of $\beta$ (see Equation (3.11)), it is not possible to choose $\alpha = 0$ to only focus on lowering

electricity cost. In practice what $\alpha = 0$ would mean for the user is the desire to have the electricity cost as low as possible. Then, the heat pump could be turned of completely. Since $\beta$ is implemented for performance, it would be possible to implement the objective function according to Equation (3.9) and use $\alpha = 0$ but then again, the MPC would always output $u = 0$ W as control signal.

### 5.6.2 Soft Constraint

When choosing the design of the soft constraint, the level of importance regarding keeping within or close to the comfort range is up to the user. Some may think it is not necessary to be within the comfort range at all cost. If the spot price would increase drastically there would be an opportunity to either raise the indoor temperature above the comfort range and/or let it sink below for some time in order to save on electricity cost. A simple way to accomplish this would be to expand the comfort range while still maintaining a large immediate penalty. The way the slack variable $\epsilon$ is used together with $R_\epsilon$ in the objective function in Equation (3.9) could also be altered in different ways. Raising it to some power other than 1 and tuning $R_\epsilon$ would provide a way to enable small penalties for indoor temperatures outside but close to the comfort range. As indoor temperature continues to deviate, the penalty rises exponentially. This could be tuned to fit the users preferences and the way the penalty is used could be done in other ways. However in this thesis, a linear penalty is used and the comfort range is set to a feasible range to use as default in a consumer product.

## 5.7 Control Signal Characteristics

The heat pump will generally operate at the lowest operational setting ($u = 700$ W). This is reasonable as the COP is the highest at this power setting (see Figure 3.5). In case the objective value is lower for other power settings those will of course be used. Here, the case $\alpha = 0.010$ is used for exemplification. The second most common power setting is $u = 0$ W, which was used between 9.5 % and 27.5 % of the time for the different periods (see Figures 4.8, 4.9, and 4.10).

It is important to note that this control signal characteristic is only optimal with regards to the objective function used in this thesis. In reality, there are more factors to be taken into account. For example, it is advantageous to reduce the amounts of starts and stops to increase the life span of the compressor. Looking at Figure 5.3, which displays $u$ during the first day of period 2, it is evident that the compressor is turned on and off repeatedly between 18:00 and 20:00. It might be possible to keep it turned off or on for longer periods of time without having a big effect on indoor temperature, which would likely be better for longevity. The compressor might also be occupied with producing hot tap water giving periods where the space heating input is forced to be 0. Expanding the objective function by introducing penalties for each start and/or stop should be simple since we are already using integer programming. It should however be noted that this would increase the model complexity which would make the optimization problem harder to solve.

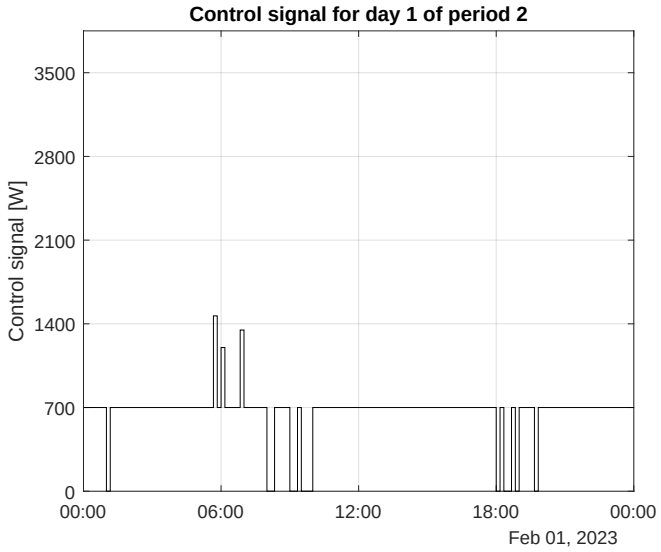


***Figure 5.3:*** *Control signal produced by the Standard MPC for day 1 of period 2.*

## 5.8 Implementation Feasibility

This thesis has only analysed the theoretical possibility of using MPC for heat pump control by simulating a system on a personal computer. Implementing the controller on a real heat pump would result in more challenges of which some are discussed in the following sections.

### 5.8.1 Heating System Model

Identifying a model of a heating system with a ground source heat pump is relatively easy once enough data has been recorded. This identification might need to be done for each specific system, as the power output at different flow temperatures differs depending on the size of the system. In the future, it would be interesting to investigate if standard heating system models can be designed for different combinations of heat pump models and size of the radiator system. This would be easier to implement commercially, as no identification of each customer heating system needs to be performed.

### 5.8.2 House Model

Modeling a house is complex. Making accurate white box models is hard and these often deviate significantly from measured values [23]. Other methods are often used instead such as RC modeling with parameter estimation. RC modeling of a house can be done with different levels of complexity. A first order and

a second order system is used in this thesis. Parameter estimation requires data from experiments for the house that is to be modeled in order to find the resistance and capacitance values. This kind of data was not available for the same house as the heat pump data was extracted from and hence external data had to be used.

### 5.8.3 Computing Power

In practical implementations, the controller for a heat pump generally runs on an embedded system with limited computing power. Running the controller developed in this thesis requires significant computing power, unlike standard heat pump controllers which might only need to perform a few floating point operations. For this reason, an important aspect in a real-world implementation will be to ensure satisfactory computing power. This ought to be possible for a few reasons. Embedded systems get more and more powerful with technical development, which speaks in favor of the future potential of high performance applications in embedded systems. The long sample time of the controller (10 min) means that there is a relatively long allowed time for each computing cycle. The nature of a heat pump means that it is not safety critical that the MPC always works. In case of failure, it could revert to, for example, a classic heat curve controller. This can be compared with, for example, steering a motor vehicle. A controller made for this purpose might have a sample time in the magnitude of milliseconds while the nature of its operation means that controller robustness is critical for safety.

### 5.8.4 Spot Price Data

In this thesis only spot price was used as the electricity price. In a real-world implementation, the specific values of the other components of the electricity price (explained in Section 2.4) would be known. It should therefore be easy to include those in the electricity price vector used during the optimization.

## 5.9 Conclusion

The problem formulation was

> *Can electricity cost for a heat pump be reduced while maintaining comfort by utilizing optimal control strategies in combination with electricity price data and weather prediction?*

The result has shown that it is possible to reduce electricity cost by utilizing MPC compared to the baseline controller. It did so by using spot price data and weather forecasts for a dynamic horizon of 12 to 36 hours. The quality of available weather forecasts are satisfactory for this purpose, although more accurate radiation forecasts would make a more precise model possible, thus further increasing the ability to maintain comfortable temperatures.

This has however been possible by allowing a deviation from reference indoor temperature. It has been assumed that the indoor temperature is comfortable if the deviation is equal to or less than 2°C. This is a subjective assessment and some people might find a deviation of 2°C uncomfortable. It is important to note that it is necessary to utilize a mass as thermal inertia in order to move power consumption in time. If the house itself is used as this thermal inertia, the temperature within the house will vary.

It is important that COP is accurately modeled. Since COP decreases when power input increases, accurate modeling of COP is essential to find the true optimal input. Using a constant COP is not good enough for a ground source heat pump as it does not capture this dynamic.

## 5.10 Future Work

In future studies there are several ways to continue on this thesis. One key aspect of this thesis is to move electricity consumption through time by using thermal inertia of buildings. Investigating how increasing the thermal inertia with, for example, a water tank would affect the results with MPC is of interest.

Additionally the focus was on electricity cost and comfort, but there are possibilities to add other factors. Total power consumption could be a suitable focus, for example when electricity availability is restricted on the grid or if you would run of a battery in which case the optimization would not need to take electricity cost into account.

Using the standard MPC controller in this thesis for implementation in a real world operating heat pump will require more work in order to minimize the risk of damaging the heat pump. It could be by implementing more rules and constraints in the controller or by adding fail safes in the heat pump. Adding complexity to the MPC could result in long computational times and a standard heat curve or a simple fallback method would be suitable. The way to do this needs further studies.

With the perspective of a heat pump manufacturer of consumer products, the tolerance of consumers regarding indoor temperature and specifically the trade-off between cost and comfort should be studied in some way. This would benefit the design of the weight $\alpha$ and the comfort range.

# Appendix

# A

# Controller Performance Plots

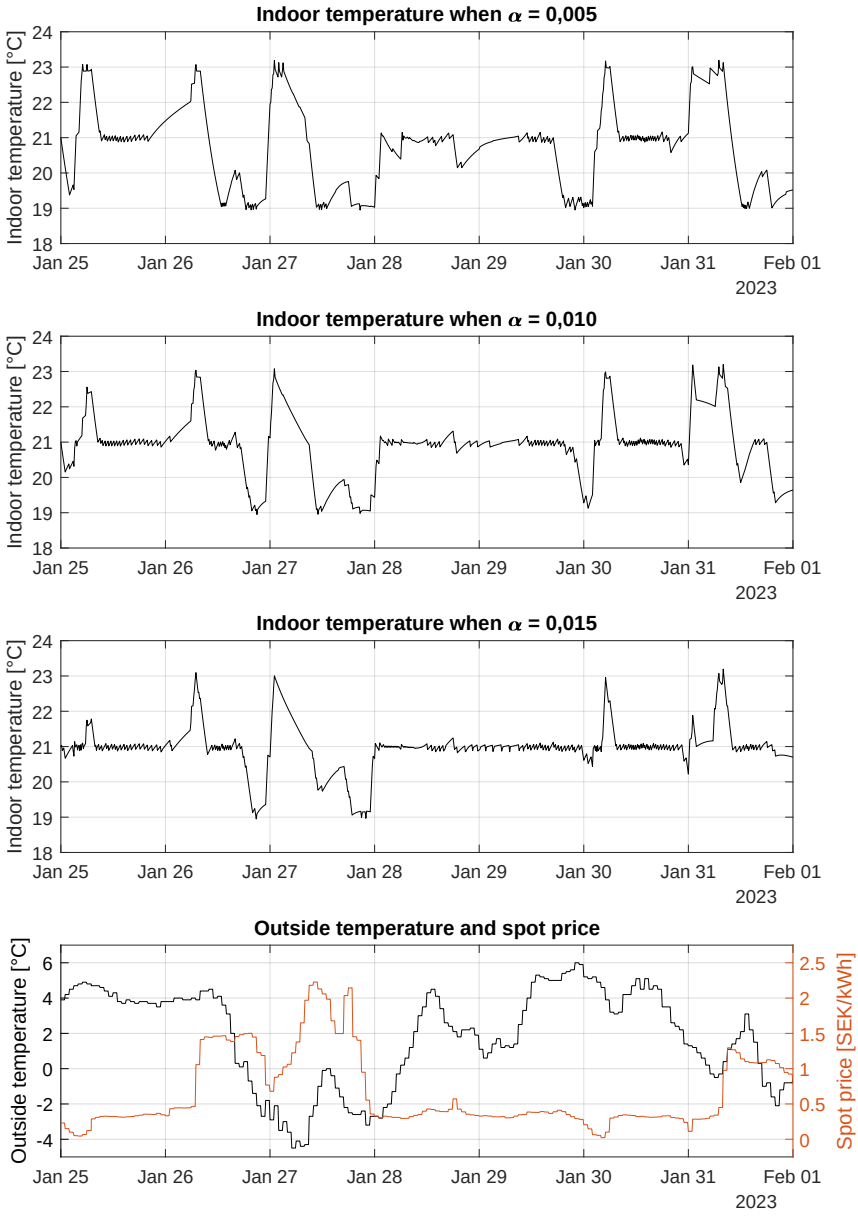


***Figure A.1:*** *Standard MPC in period 1.*

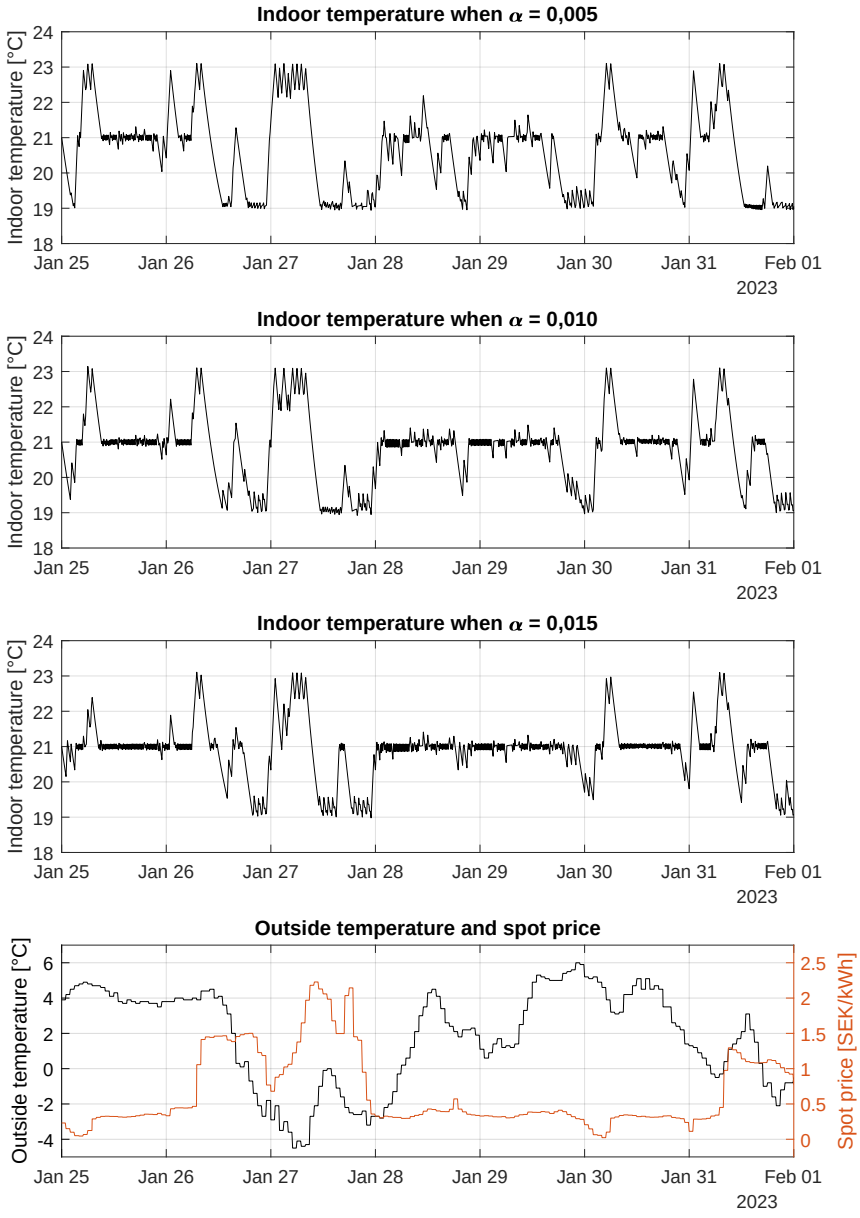


***Figure A.2:*** *Constant COP MPC in period 1.*

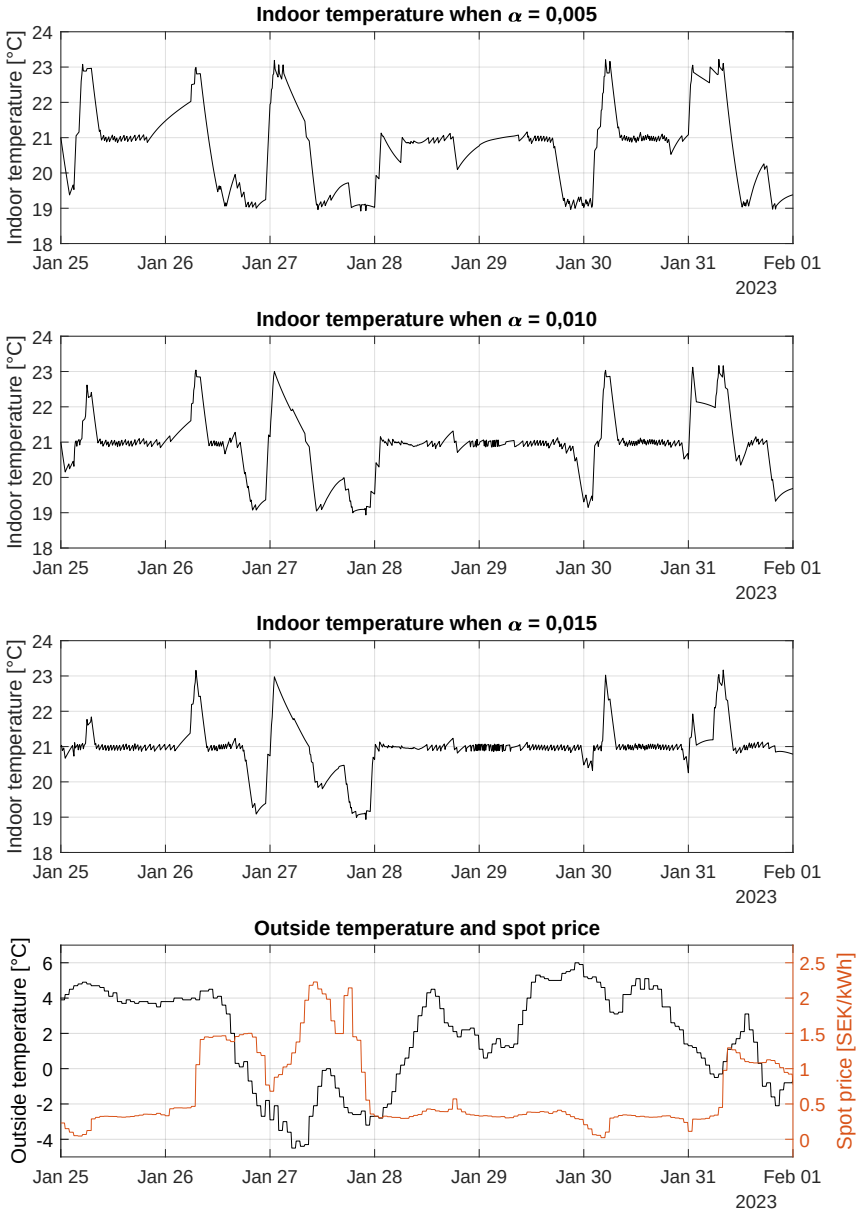


***Figure A.3:*** *Perfect prediction MPC in period 1.*

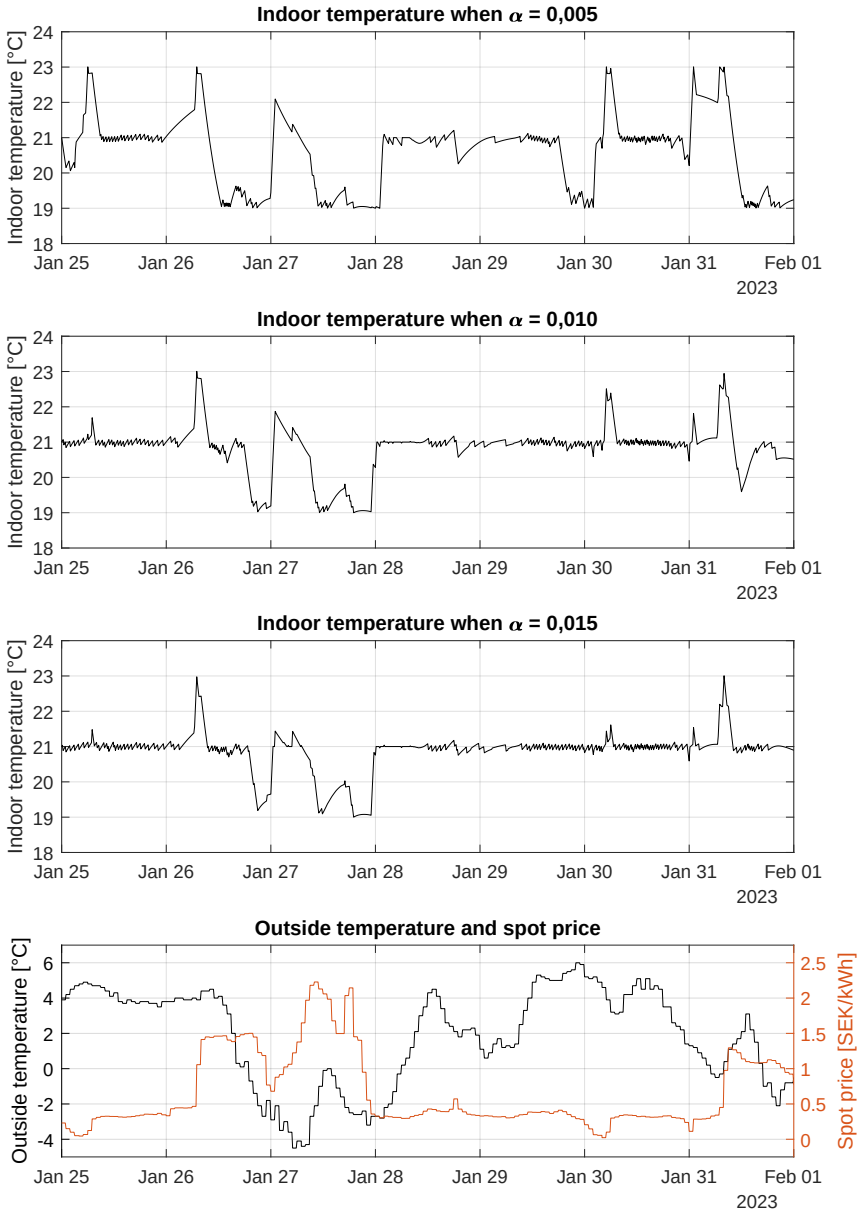


***Figure A.4:*** *Oracle MPC in period 1.*

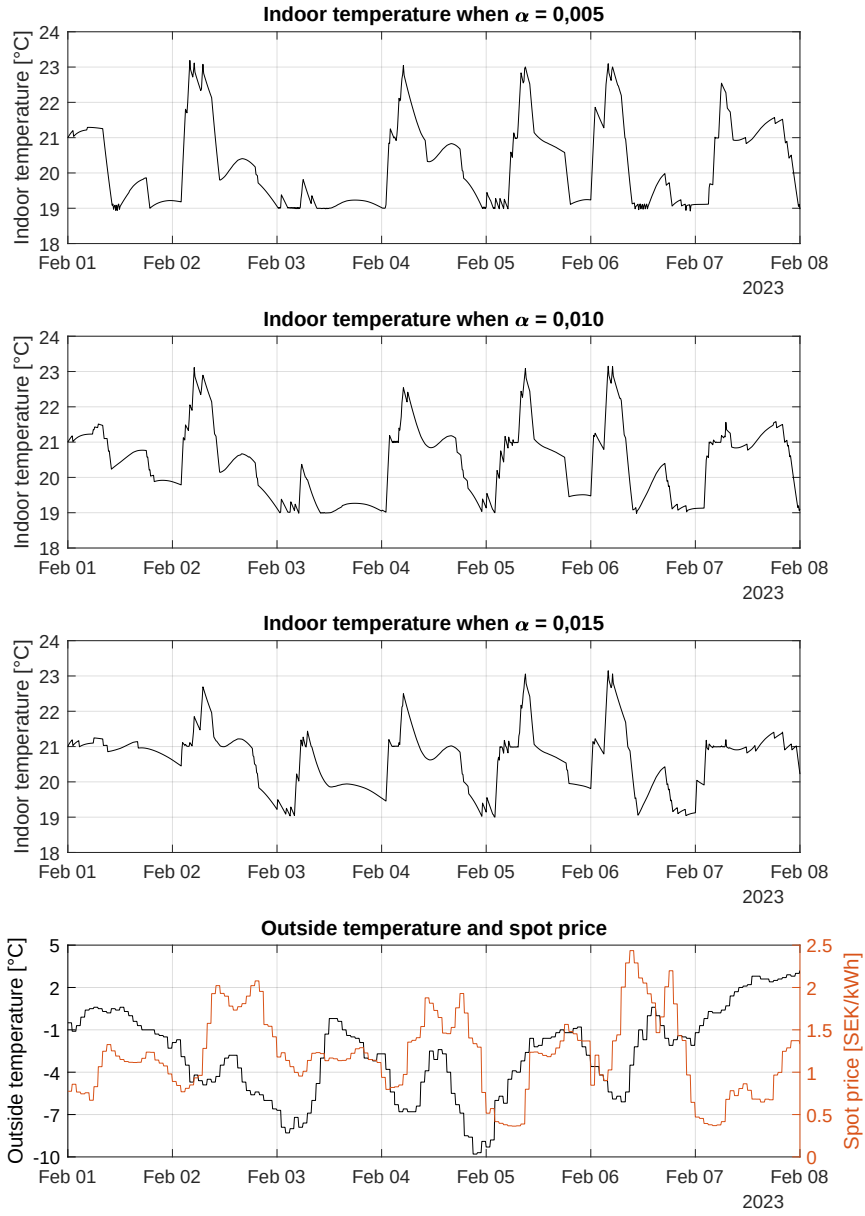


***Figure A.5:*** *Standard MPC in period 2.*

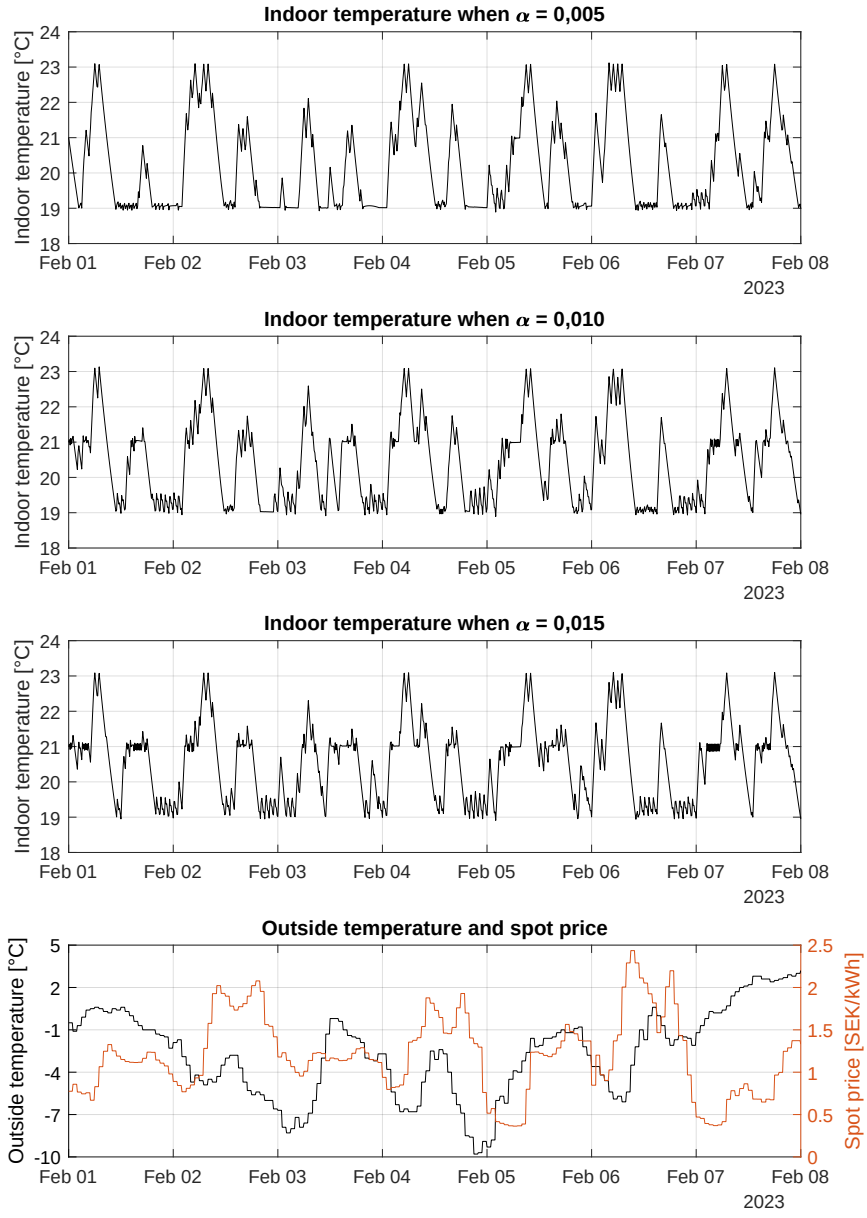


***Figure A.6:*** *Constant COP MPC in period 2.*

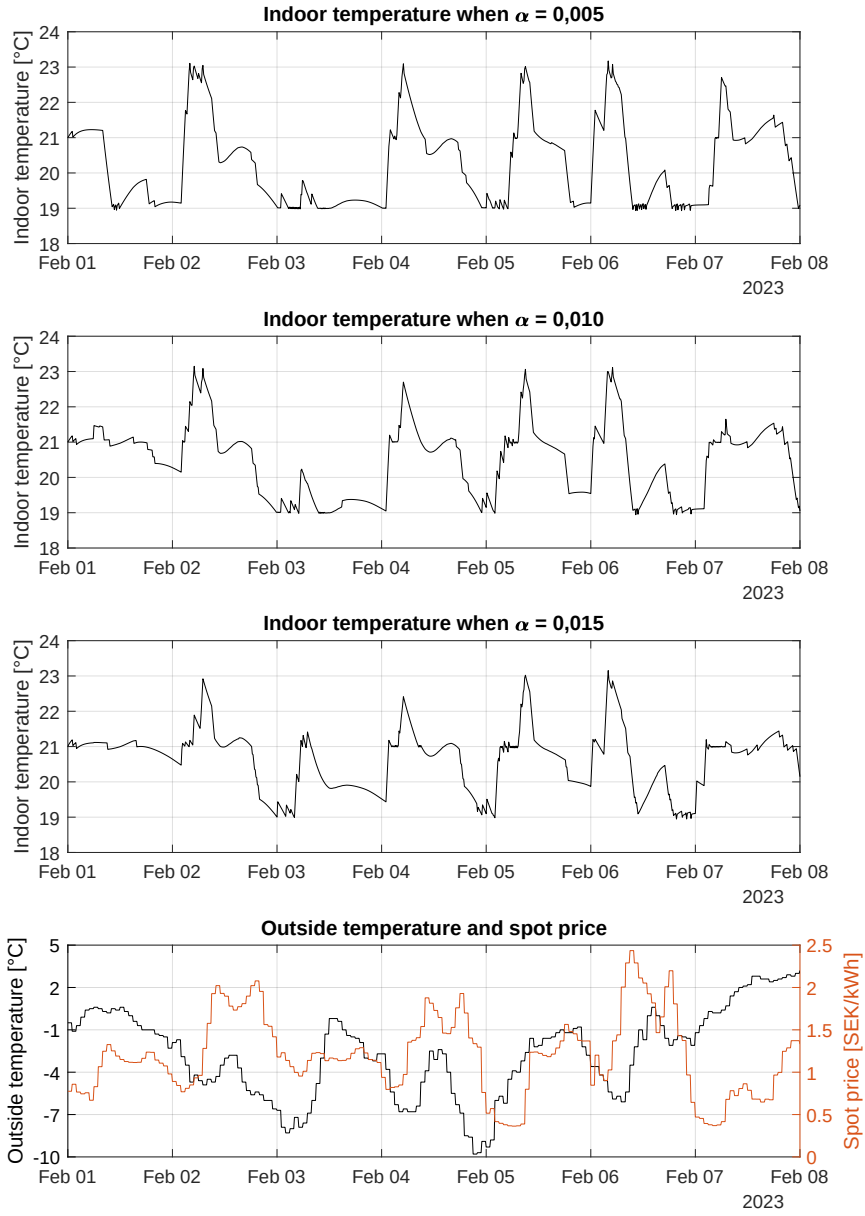


***Figure A.7:*** *Perfect prediction MPC in period 2.*

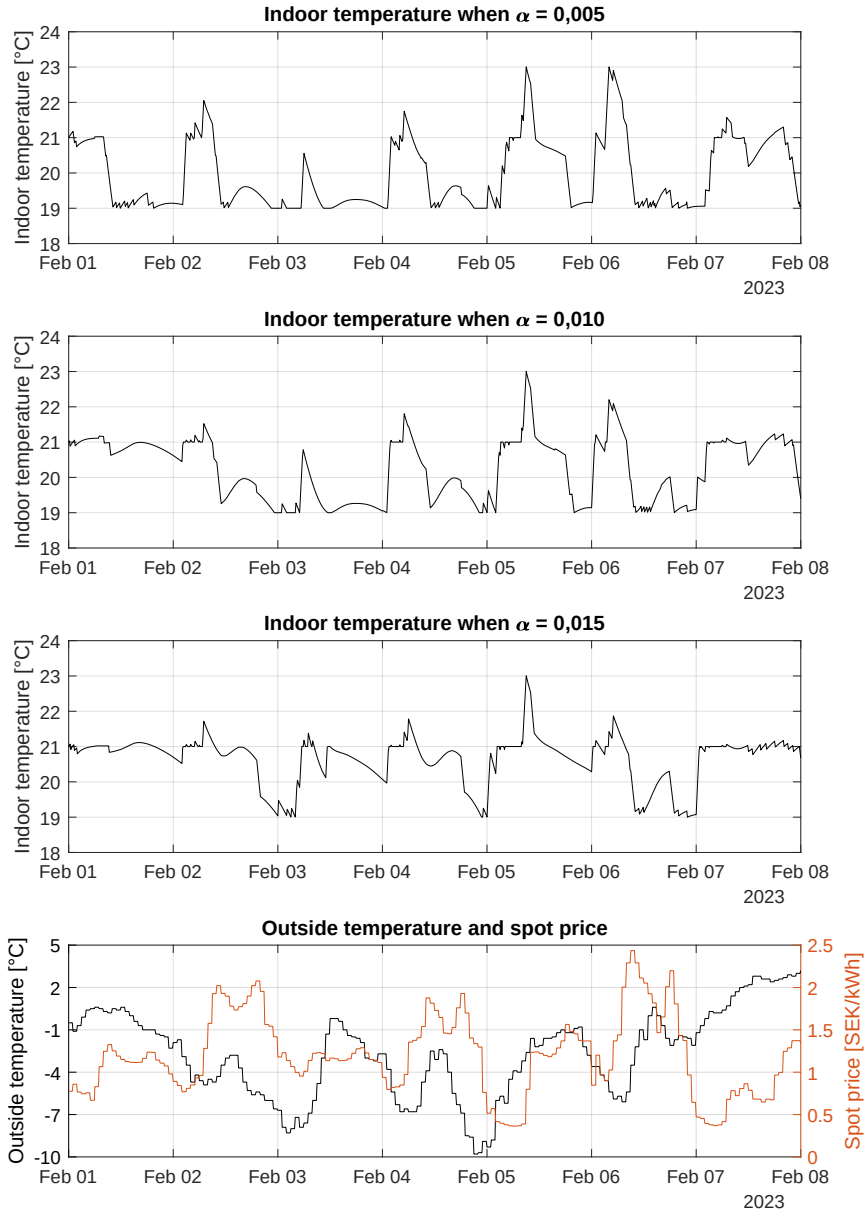


***Figure A.8:*** *Oracle MPC in period 2.*

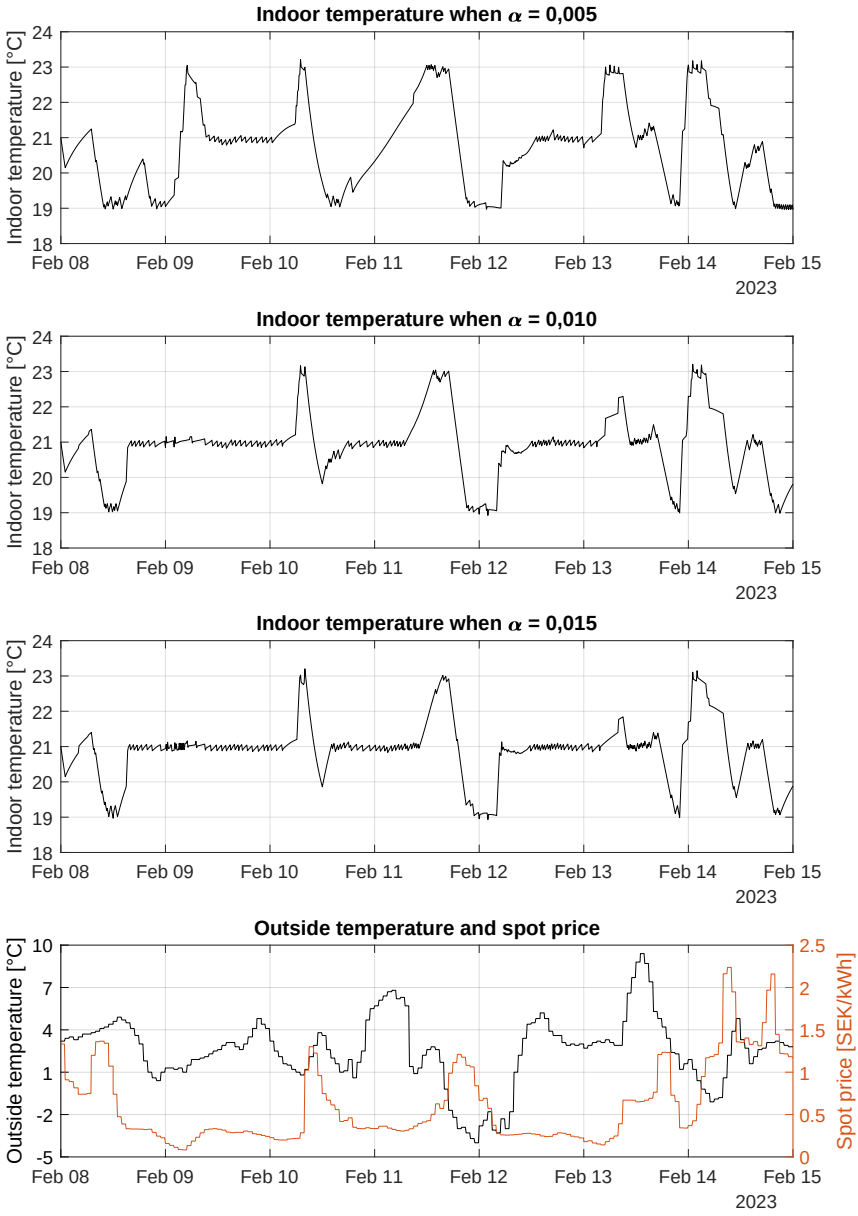


***Figure A.9:*** *Standard MPC in period 3.*

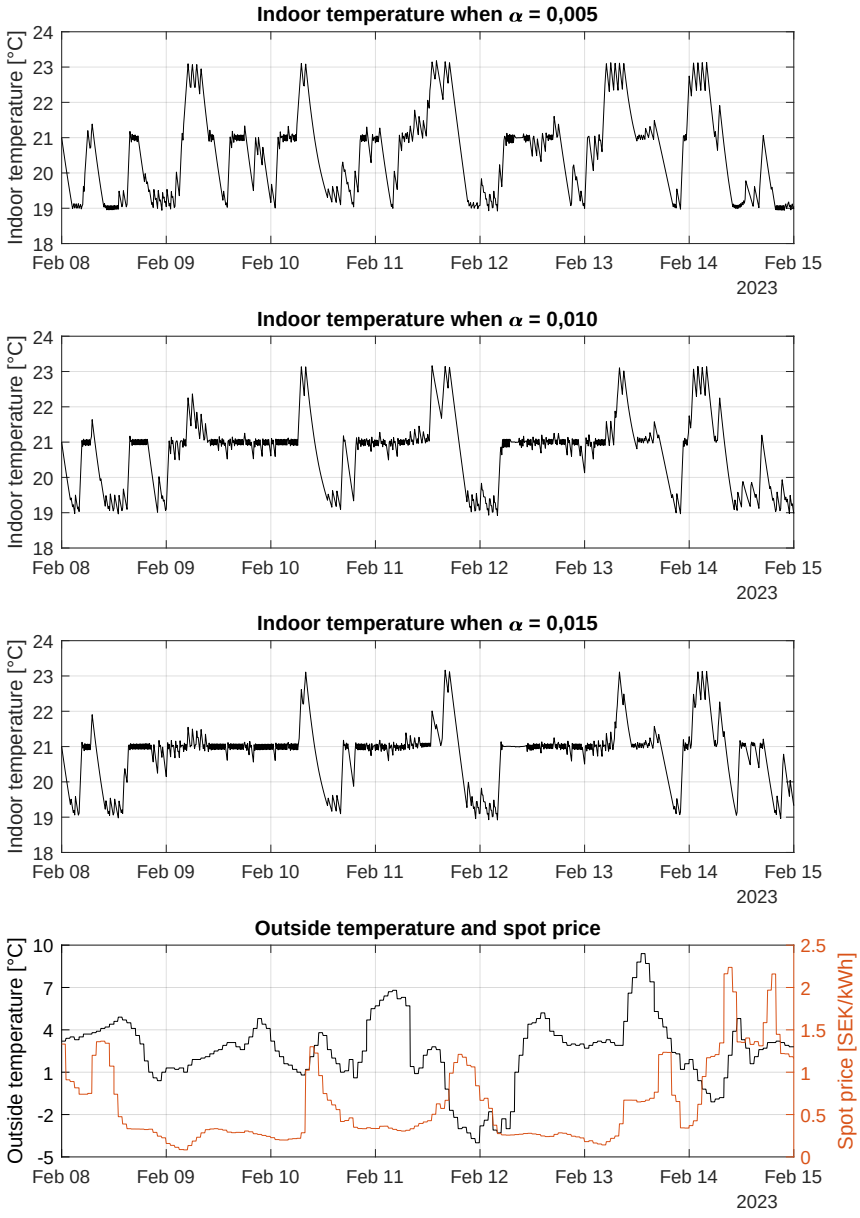


***Figure A.10:*** *Constant COP MPC in period 3.*

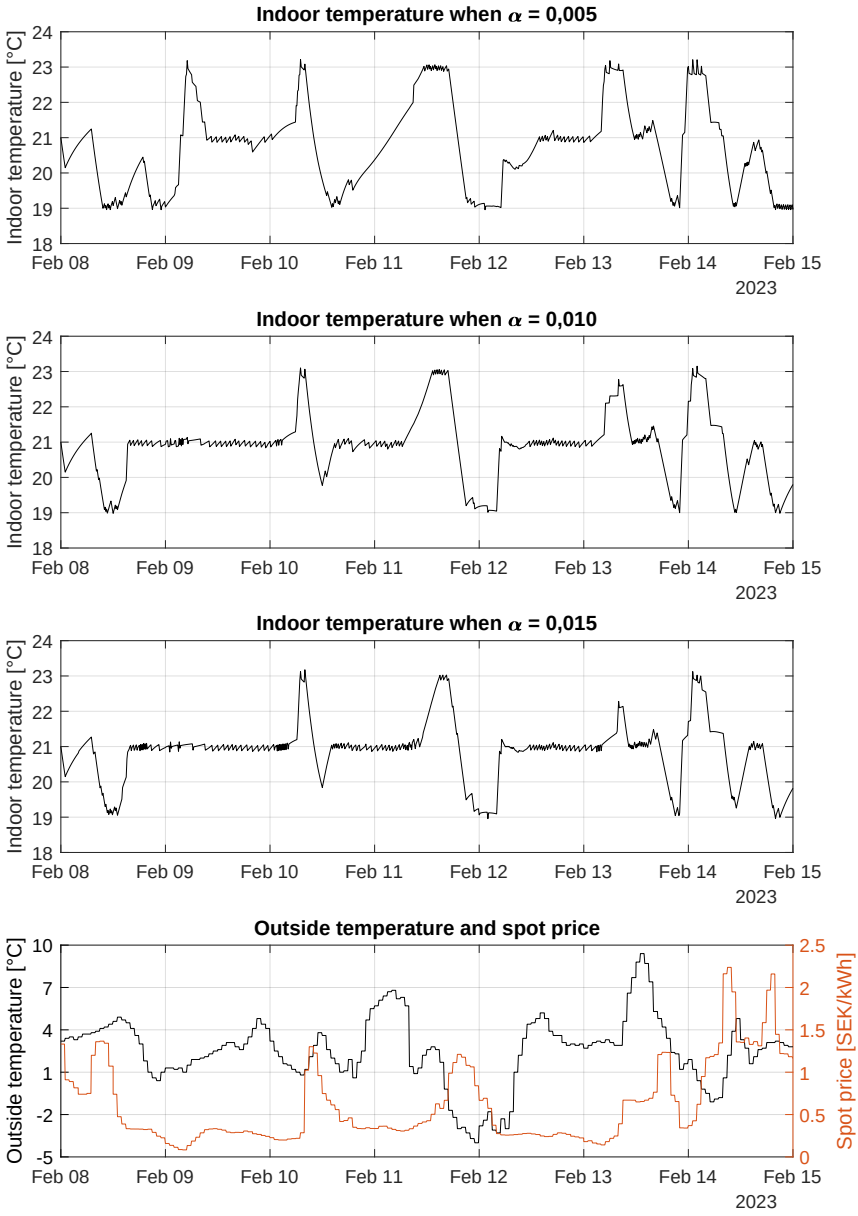


***Figure A.11:*** *Perfect prediction MPC in period 3.*

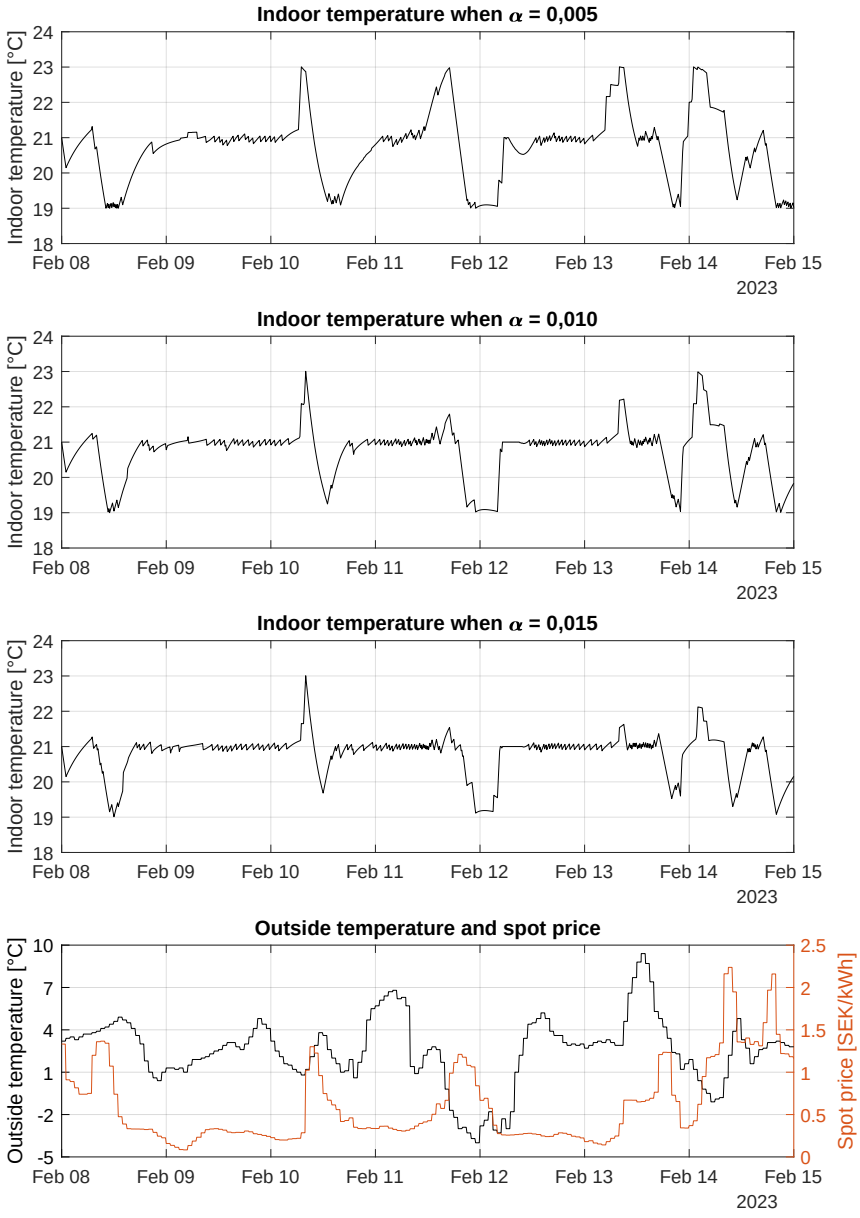


***Figure A.12:*** *Oracle MPC in period 3.*

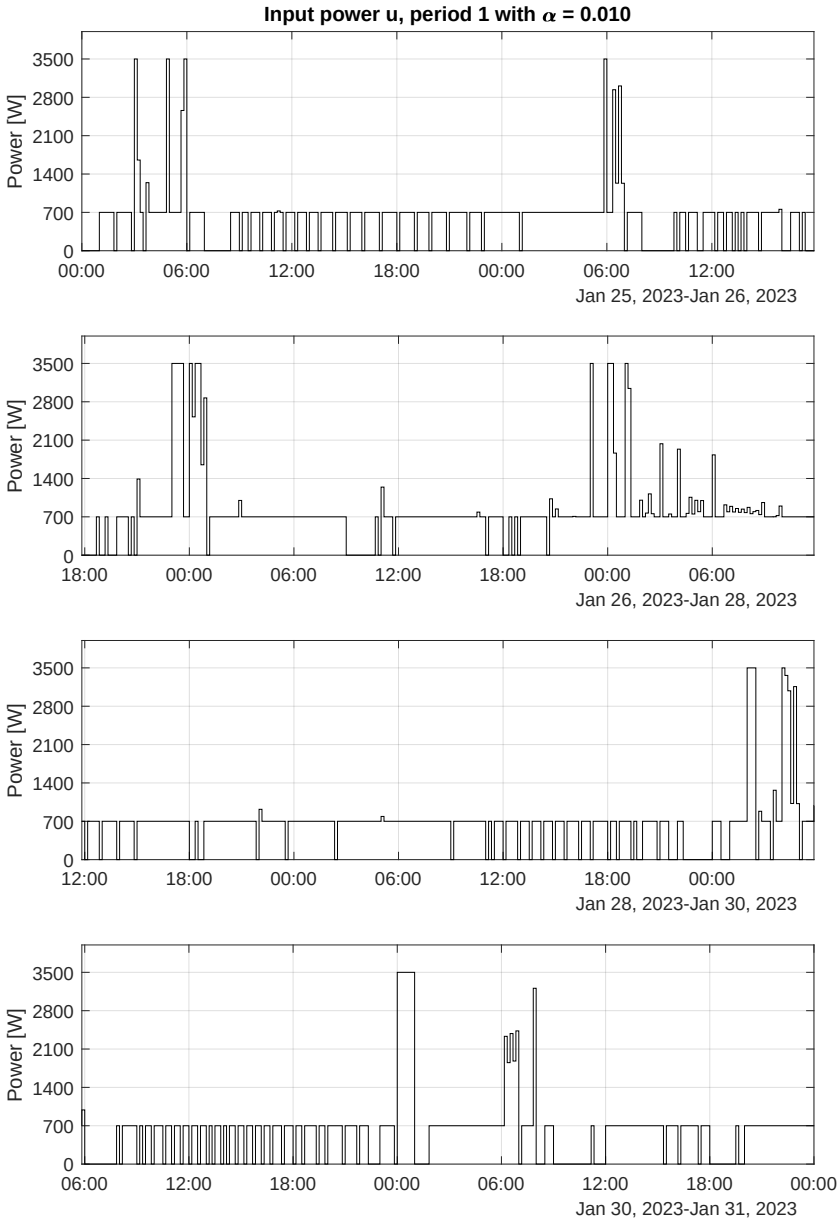


***Figure A.13:*** *Input power u for the standard MPC controller during period 1 with* $\alpha = 0.010$.

# B

# Radiation Model

As radiation is taken into account in the house model, it would be advantageous to accurately predict future radiation. As radiation is not specified in SMHI's forecasts, models for estimating radiation as a function of sunshine and cloudiness are independently developed. However, the inverse correlation between cloudiness (which is what is specified in SMHI's forecasts) and sunshine (and thereby radiation) is low. Therefore radiation forecasts are not taken into account in the MPC. The results of the developed model are however still found interesting by the authors and are therefore presented here.

## B.1 Radiation as a Function of Sunshine

There are historical records for radiation and sunshine. This means that the correlation between sunshine and radiation can be investigated. Global radiation is recorded in the unit $W/m^2$, while sunshine is recorded as *seconds of sunshine per hour*, i.e. for every hour sunshine is specified as a value in the range of 0 to 3600. The recorded values for sunshine are normalised by dividing the data by 3600, thus for every hour sunshine is specified in a range from 0 to 1.

A hypothesis is made that radiation is mainly a function of sunshine, day of the year, and time of the day. It is assumed that the relationship between radiation and time of year and time of day is sinusoidal, due to the sinusoidal relationship between these variables and the height of the sun above the horizon. Further, it is assumed that the global radiation can never be negative, in accordance with the recorded values. The model is presented in Equation (B.1). The parameters $c_1 - c_6$ are estimated by solving the equation in a least squares sense with a set of recorded data for radiation and sunshine.

$$\hat{G} = max\Big(0,\ (S + c_1)\Big(c_2\ sin\ \Big((d + c_3)\frac{2\pi}{365}\Big) sin\Big((t + c_4)\frac{2\pi}{86400}\Big) + c_5\ sin\ \Big((d + c_3)\frac{2\pi}{365}\Big) + c_6\ sin\Big((t + c_4)\frac{2\pi}{86400}\Big)\Big)\Big) \tag{B.1}$$

where

$$\begin{aligned} S\ [-] &: \text{sunshine} \in [0, 1] \\ d\ [day] &: \text{day of year} \in \{1, 2, \ldots, 365\} \\ t\ [s] &: \text{time of day} \in \{0, 3600, 7200, \ldots, 86400\} \\ c_{1-6}\ [-] &: \text{Model parameters} \in \mathbb{R} \end{aligned}$$

#### Estimation and validation

Data from 2020-01-01 to 2020-12-31 is used for estimation and data from 2021-01-01 to 2021-12-31 is used for validation. The parameter estimation using the least square method yields the values in Table B.1. Figure B.1 showcases a comparison between measured values and the model for the validation data. The validation shows a mean average error (MAE) 15,7 and a root mean square error (RMSE) 30,5.

***Table B.1:*** *Radiation as a function of sunshine, model parameters*

| Parameter | Value |
|---|---|
| $c_1$ | 0.4743 |
| $c_2$ | 29.0431 |
| $c_3$ | -79.1320 |
| $c_4$ | -19626.3586 |
| $c_5$ | 209.0901 |
| $c_6$ | 341.8058 |

## B.2 Radiation as a Function of Cloudiness

Four measurements of cloudiness are specified in each forecast; mean values for *low*, *medium*, and *high* level cloudiness as well as mean values for *total* cloud coverage. Total cloud coverage is used here. Cloudiness is specified in each forecast as an integer between 0 and 8, where 0 means that the sky is completely clear and 8 means that there is complete cloud coverage. Measured values of total cloud coverage is specified in the range 0 % to 100 %. Sometimes if the cloud coverage cannot be determined due to fog, precipitation or if the sight is reduced for other reasons, the value is set at 113 %. As the global radiation is assumed to be very

low in these cases those recordings are left at 113 %. This data is normalised between 0 and 1 (with a few values of 1.13) by division with 100.

A similar model as was defined in B.1 is defined again. The same hypothesis is used, although it is assumed that cloudiness is inversely correlated with radiation. The parameters $c_2$, $c_6$ and $c_8$ are added as this yields a better fit when using the least squares method.

$$\begin{aligned}\hat{G} = max\Big(0,\ (c_1 - C)\Big(c_2 + c_3\ sin\ \Big((d + c_4)\frac{2\pi}{365}\Big) sin\Big((t + c_5)\frac{2\pi}{86400}\Big)\\ + c_6 + c_7\ sin\ \Big((d + c_4)\frac{2\pi}{365}\Big)\\ + c_8 + c_9\ sin\Big((t + c_5)\frac{2\pi}{86400}\Big)\Big)\Big)\end{aligned} \tag{B.2}$$

where

$$\begin{aligned} C\ [-] &: \text{cloudiness} \in \{[0, 1], 1.13\}\\ d\ [day] &: \text{day of year} \in \{1, 2, \ldots, 365\}\\ t\ [s] &: \text{time of day} \in \{0, 3600, 7200, \ldots, 86400\}\\ c_{1-9}\ [-] &: \text{Model parameters} \in \mathbb{R}\end{aligned}$$

### Estimation and validation

Data from 2020-01-01 to 2020-12-31 is used for estimation and data from 2021-01-01 to 2021-12-31 is used for validation. The parameter estimation using the least square method yields the values in Table B.2. Figure B.2 showcases a comparison between measured values and the model for the validation data. The validation shows a mean average error (MAE) 54.0 and a root mean square error (RMSE) 112.2.

***Table B.2:*** *Radiation as a function of cloudiness, model parameters*

| Parameter | Value |
|---|---|
| $c_1$ | 1.8873 |
| $c_2$ | -106.6655 |
| $c_3$ | 24.7081 |
| $c_4$ | -77.6313 |
| $c_5$ | -19414.6441 |
| $c_6$ | -38948.4021 |
| $c_7$ | 168.9647 |
| $c_8$ | 39041.3479 |
| $c_9$ | 261.7216 |

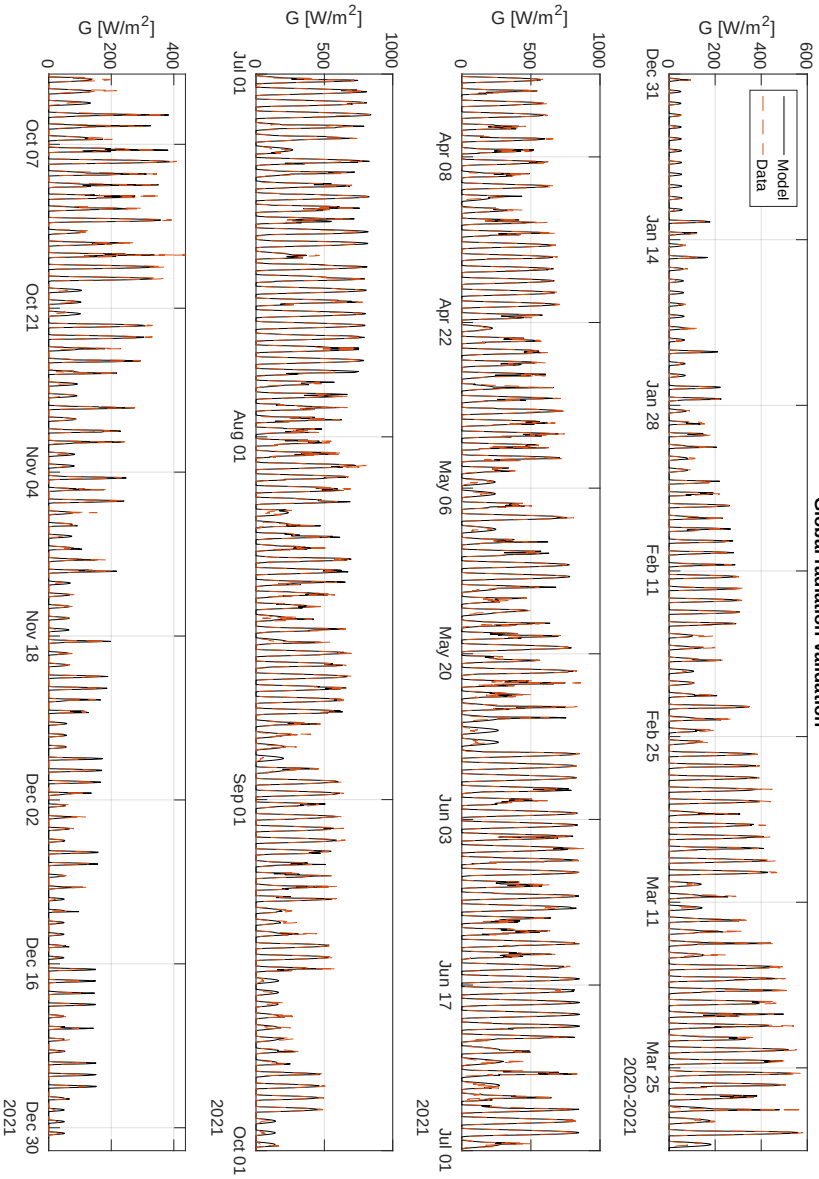


***Figure B.1:*** *Validation of $\hat{G} = f(S)$ model using data from the entire year of 2021.*


***Figure B.2:*** *Validation of $\hat{G} = f(C)$ model using data from the entire year of 2021.*

# Bibliography


[1] European Commission. Nationally Determined Contribution of the European Union and its Member States, December 2020. URL https://unfccc.int/sites/default/files/NDC/2022-06/EU_NDC_Submission_December%202020.pdf.

[2] Statistiska Centralbyrån. Elproduktion och förbrukning i Sverige, November 2022. URL https://www.scb.se/hitta-statistik/sverige-i-siffror/miljo/elektricitet-i-sverige/. Accessed: 2023-05-12.

[3] Clean Energy Wire. Setting the power price: the merit order effect, January 2015. URL https://www.cleanenergywire.org/factsheets/setting-power-price-merit-order-effect. Accessed: 2023-01-18.

[4] Energimyndigheten. Ny statistik över Energianvändningen i småhus, flerbostadshus och lokaler, May 2022. URL https://www.energimyndigheten.se/statistik/den-officiella-statistiken/statistikprodukter/energistatistik-for-smahus/. Accessed: 2023-01-18.

[5] Kristian Huchtemann. *Supply temperature control concepts in heat pump heating systems*. PhD thesis, RWTH Aachen University, Aachen, May 2015.

[6] Sarah Noye, Rubén Mulero Martinez, Laura Carnieletto, Michele De Carli, and Amaia Castelruiz Aguirre. A review of advanced ground source heat pump control: Artificial intelligence for autonomous and adaptive control. *Renewable and Sustainable Energy Reviews*, 153:111685, January 2022.

[7] Mikkel Urban Kajgaard, Jesper Mogensen, Anders Wittendorff, Attila Todor Veress, and Benjamin Biegel. Model predictive control of domestic heat pump. In *2013 American Control Conference*, pages 2013–2018, Washington DC, USA, June 2013.

[8] Recep Yumrutaş and Mazhar Ünsal. Energy analysis and modeling of a solar assisted house heating system with a heat pump and an underground energy storage tank. *Solar Energy*, 86(3):983–993, March 2012.

[9] Pin Wu, Zhichao Wang, Xiaofeng Li, Zhaowei Xu, Yingxia Yang, and Qiang Yang. Energy-saving analysis of air source heat pump integrated with a water storage tank for heating applications. *Building and Environment*, 180: 107029, August 2020.

[10] NIBE Energy Systems. Vad är Smart Price Adaption (SPA)? URL `https://www.nibe.eu/sv-se/support/vanliga-fragor/faq-items/vad-ar-smart-price-adaption-spa`. Accessed: 2023-05-11.

[11] Frauke Oldewurtel, Alessandra Parisio, Colin N. Jones, Dimitrios Gyalistras, Markus Gwerder, Vanessa Stauch, Beat Lehmann, and Manfred Morari. Use of model predictive control and weather forecasts for energy efficient building climate control. *Energy and Buildings*, 45:15–27, February 2012.

[12] Jan Široký, Frauke Oldewurtel, Jiří Cigler, and Samuel Prívara. Experimental analysis of model predictive control for an energy efficient building heating system. *Applied Energy*, 88(9):3079–3087, September 2011.

[13] Samuel Prívara, Jiří Cigler, Zdeněk Váňa, Frauke Oldewurtel, Carina Sagerschnig, and Eva Žáčeková. Building modeling as a crucial part for building predictive control. *Energy and Buildings*, 56:8–22, January 2013.

[14] Yunus A. Çengel, John M. Cimbala, and Robert H. Turner. *Fundamentals of Thermal-Fluid Sciences*. McGraw-Hill Education, 5 edition, 2017.

[15] NIBE Energy Systems. Ground source heat pump NIBE S1255 Product leaflet. Technical report, 2022.

[16] Swedish Standards Institute. SS-EN 14825:2022. Air conditioners, liquid chilling packages and heat pumps, with electrically driven compressors, for space heating and cooling, commercial and process cooling – Testing and rating at part load conditions and calculation of seasonal performance. Stockholm. 2022.

[17] Magnus Thorstensson. Elmarknadsstatistik, February 2017. URL `https://www.energiforetagen.se/statistik/statistik-i-bilder/Elmarknadsstatistik/`. Accessed: 2023-05-05.

[18] Energimarknadsinspektionen. EIFS 2022:1 - Energimarknadsinspektionens föreskrifter och allmänna råd för utformning av nättariffer för ett effektivt utnyttjande av elnätet, March 2022.

[19] Nord Pool. Nord Pool Day-Ahead, January 2023. URL `https://www.nordpoolgroup.com/en/Market-data1/Dayahead/Area-Prices/ALL1/Hourly/`. Accessed: 2023-01-18.

[20] Torkel Glad and Lennart Ljung. *Reglerteori - Flervariabla och olinjära metoder*. Studentlitteratur AB, Lund, 2 edition, 2003.

[21] Johan Löfberg. YALMIP : A Toolbox for Modeling and Optimization in MATLAB. In *In Proceedings of the CACSD Conference*, Taipei, Taiwan, 2004.

[22] NIBE Energy Systems. Technical Manual - NIBE VVM 320. Technical report, 2020.

[23] K. A. Antonopoulos and E. Koronaki. Apparent and effective thermal capacitance of buildings. *Energy*, 23(3):183–192, March 1998.